05 Jun 2021

A Review On Alpha Case Formation And Modeling Of Mass Transfer During Investment Casting Of Titanium Alloys

R. Sharon Uwanyuze
Missouri University of Science and Technology, ruvhg@mst.edu

Janos E. Kanyo

Sarah F. Myrick

Stefan Schafföner

Recommended Citation

R. S. Uwanyuze et al., "A Review On Alpha Case Formation And Modeling Of Mass Transfer During Investment Casting Of Titanium Alloys," *Journal of Alloys and Compounds*, vol. 865, article no. 158558, Elsevier, Jun 2021.
The definitive version is available at https://doi.org/10.1016/j.jallcom.2020.158558

Journal of Alloys and Compounds 865 (2021) 158558

Contents lists available at ScienceDirect

Journal of Alloys and Compounds

journal homepage: www.elsevier.com/locate/jalcom

Review

A review on alpha case formation and modeling of mass transfer during investment casting of titanium alloys

R. Sharon Uwanyuze[a], Janos E. Kanyo[a], Sarah F. Myrick[b], Stefan Schafföner[a,c,*]

[a] Department of Materials Science and Engineering, University of Connecticut, Storrs, CT 06269, USA
[b] Department of Biomedical Engineering, University of Connecticut, Storrs, CT 06269, USA
[c] Institute of Materials Science, University of Connecticut, Storrs, CT 06269, USA

ARTICLE INFO

Article history:
Received 4 November 2020
Received in revised form 26 December 2020
Accepted 28 December 2020
Available online 5 January 2021

Keywords:
Titanium alloys
Investment casting
Mass transfer
Metal-mold reactions
Refractories
Corrosion
alpha-case

ABSTRACT

Titanium alloys have excellent corrosion resistance, high temperature strength, low density, and biocompatibility. Therefore, they are increasingly used for aerospace, biomedical, and chemical applications. Investment casting is a well-established process for manufacturing near-net-shape intricate parts for such applications. However, mass transfer arising from metal-mold reactions is still a major problem that drastically impairs the surface and properties of the castings. Although there have been astounding developments over the past 20 years, they remain scattered in various research papers and conference proceedings. This review summarizes the current status of the field, gaps in the scientific understanding, and the research needs for the expansion of efficient casting of titanium alloys. The uniqueness of this paper includes a comprehensive analysis of the interfacial reactions and mass transfer problems. Additionally, momentum and heat transfer are presented where applicable, to offer a holistic understanding of the transport phenomena involved in investment casting. Solutions based on modeling and experimental validation are discussed, highlighting ceramic oxide refractories like zirconia, yttria, calcia, alumina, and novel refractories namely, calcium zirconate and barium zirconate. It was found that while mold material selection is vital, alloy composition should also be carefully considered in mitigating metal-mold reactions and mass transfer.

Contents

* Corresponding author.
E-mail address: stefan.schaffoener@uconn.edu (S. Schafföner).

https://doi.org/10.1016/j.jallcom.2020.158558
0925-8388/

1. Introduction

With increased global connection through aviation, and groundbreaking advancements in biomedical implants, lightweight and corrosion-resistant alloys are needed more than ever. In the aerospace industry, low density alloys are needed to reduce noise and minimize fuel consumption [1]. As a case in point, the international civil aviation organization (ICAO) has a current goal of a 50% reduction in emissions by 2050 [2]. The high strength-to-weight ratio of titanium alloys, makes them exceptionally attractive for aerospace applications. Furthermore, titanium alloys can be applied at higher temperatures than common lightweight alloys like aluminum and magnesium alloys as demonstrated in Fig. 1 [3,4]. Titanium alloys maintain their high temperature strength up to 600 °C, and advanced titanium alloys like γ-TiAl and Ti-Nb-Mo have exceptional creep resistance up to 750 °C [5]. In addition to ambient and high temperature capabilities, some alpha-titanium alloy such as Ti-5Al-2.5Sn can also withstand cryogenic temperatures, while maintaining excellent fracture toughness and elongation [6].

Another major application of titanium alloys is in the biomedical industry. A literature survey showed that 70–80% of implants are made from metallic biomaterials [7], indicating the high demand for biocompatible, lightweight, and corrosion-resistant alloys that integrate well in the body. Titanium alloys have excellent biocompatibility and specific strength which are superior to their counterparts—316L stainless steel and cobalt-chromium alloys [7–9]. Additionally, β-titanium alloys like Ti-29Nb-13Ta-4.6Zr (TNTZ) have a notably comparable Young's modulus to human bone [10]. Therefore, it is not surprising that titanium alloys are frequently used for orthopedic, dental and cardiovascular implants [11]. Care has to be taken, however, when alloying titanium for implant applications because mass transfer of elemental ions—particularly aluminum and vanadium—has been linked to long-term nerve damage and Alzheimer's disease [12,13]. Oxidation heat treatments or application of ceramic coatings are some of the current ways to mitigate surface mass transfer and improve wear resistance of titanium alloys [14–16]. For example, Ti-6Al-7Nb alloy oxidized at 800 °C for 72 h had six times higher wear resistance than non-oxidized Ti-6Al-7Nb [16].

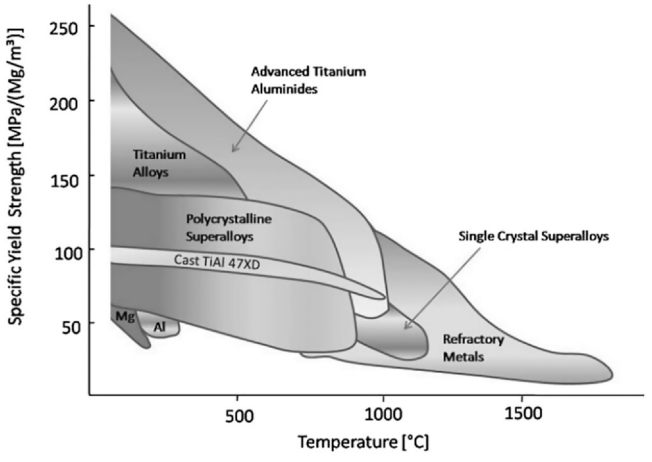

Fig. 1. Comparison of the specific yield strength of titanium alloys to that of other structural metals for aerospace applications (reprinted with permission from Ref. [3]). It can be seen that the strength-to-weight ratio of titanium alloys is superior to that of magnesium alloys, aluminum alloys, refractory metals and superalloys.

While there are different techniques to manufacture titanium alloy parts, this paper focuses on the well-established technique of investment casting. Investment casting—also known as lost wax casting—is a manufacturing method used to produce parts with complex shapes and precise dimensions at a low scrap rate and relatively low cost [17,18]. Investment casting is carried out in ceramic shell molds and is preceded by melting the titanium alloy in a water-cooled copper crucible [19,20]. Nonetheless, current studies are investigating the use of ceramic refractory crucibles to promote energy efficiency to and increase the melting volume [21–24]. A ceramic material that is corrosion-resistant as a crucible makes a viable mold. Yet, a material that corrodes during melting may still be applicable as a mold material because of the shorter contact time and lower temperature during casting compared to melting [25]. Factors that influence metal-mold reactions thus include (i) composition of the mold, (ii) mold preheat temperature, (iii) composition of the alloy, (iv) pouring temperature, (v) solidification time, and (vi) thickness of the cast part [26–30].

A major problem in investment casting of titanium alloys is mass transfer of elements such as oxygen, carbon, nitrogen, aluminum or silicon from the ceramic mold into the alloy as it solidifies, forming a subsurface layer known as alpha case (α-case) [27,29,31–33]. This layer forms during casting, annealing and other high temperature thermal-mechanical processes, but it should be distinguished from an oxygen-rich layer (ORL) that forms during service at temperatures less than 650 °C [34]. Unlike the ORL, the α-case forms upon cooling from a temperature above the β transus. At ambient temperature, the alloy surface is highly enriched with α phase and this significantly alters the surface microstructure from the bulk [34–38]. The difference between the α-case layer and the ORL is depicted in Fig. 2 for the titanium alloys Ti-6Al-4V and Ti-6242S [34]. Interestingly, controlled oxygen diffusion into the surface of titanium alloys, typically by thermal oxidation heat treatment, can significantly protect from wear and tribocorrosion [39–41]. However, during investment casting, metal-mold reactions make it a challenge to control the thickness and composition of the α-case layer [31,32,42,43]. The α-case layer significantly decreases ductility, fracture toughness and fatigue life of the casting [44,45], so there are various methods for removing it including grinding, laser irradiation, water jetting, cathodic de-oxygenation, and chemical milling [46–50]. To limit post-casting treatments and the associated costs, it is important to understand this mass transfer problem, which would also enhance near-net shape casting capabilities for titanium alloys.

The objective of this review is to analyze various models in predicting mass transfer, especially from metal-mold reactions, so as

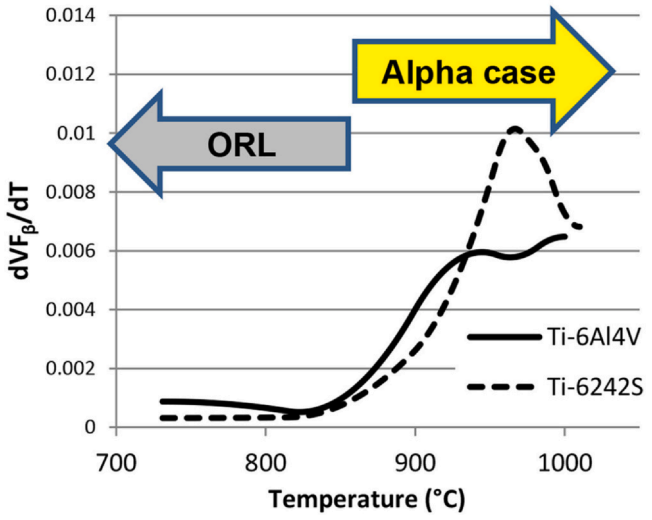

Fig. 2. Defining difference between an oxygen-rich layer and an α-case layer, based on temperature and rate of change in volume fraction of the β titanium phase. For Ti-6Al-4V and Ti-6424S, the differentiating threshold is around 850 °C (reprinted with permission from Ref. [34]).

to achieve an improved microstructure and properties of cast titanium alloy parts. Understanding the extent of the formed diffusion layer during investment casting can greatly aid industry personnel in determining how much post-casting treatment is required if any. Current solutions for addressing this mass transfer problem are investigated, which can be categorized into three sectors—using specialized equipment with a controlled melting atmosphere, improving crucible/mold materials, and post-casting machining. Various ceramic mold refractories are explored including calcia, zirconia, alumina, yttria and state-of-the-art alkaline earth ceramics (calcium zirconate and barium zirconate) to understand and compare their corrosion resistance in contact with titanium alloy melts. This review is divided into four main sections: (i) investment casting process and modeling, (ii) effect of mass transfer on microstructure and properties, (iii) methods of mitigating mass transfer, and (iv) future prospects and concluding remarks.

2. Investment casting process and modeling

Investment casting of titanium parts is performed in five main stages: pattern making, mold making, casting, divesting and surface finishing. The purpose of this work is to model the transport phenomena involved in investment casting of titanium alloys, regardless of their end application, and to predict and mitigate the negative impact of metal-mold reactions on the microstructure and properties of the casting.

2.1. Materials and equipment

Investment patterns are typically made from wax, but recently, the use of plastics/polymers has increased for rapid prototyping with additive manufacturing [51,52]. The pattern material has to be carefully chosen to ensure that its coefficient of thermal expansion is appropriate for the chosen ceramic material, otherwise, it will induce high thermal stresses in the ceramic shell during firing and lead to subsequent cracking [53]. Mold materials include zirconia, alumina, yttria, calcia, and more recently, calcium zirconate and barium zirconate [21,22,54,55]. Synthetic polymer fibers are typical reinforcements for ceramic shell molds, but lately natural alternatives like coconut fibers and rice husks were investigated because they are less costly and more sustainable [17,56].

Among mold binders, colloidal silica is common because it is environmentally safer than alcohol-based binders such as ethyl-silicate [57]. Moreover, colloidal silica showed a higher bonding strength compared to clays like bentonite [56]. Nonetheless, the silicon from silica-based binders remains in the mold, and has shown to impair the corrosion resistance of molds in contact with titanium alloy melts [58,59]. Therefore, a novel silica-free, water-based system was presented, which was comprised of xanthan gum and food grade guar gum as stabilizers and an aqueous urethane-acrylate dispersion acting as a temporary binder [60–62].

In addition to commercially pure titanium (cp-Ti), predominantly used titanium alloys include Ti-6Al-4V, Ti-Al and Ti-Nb [5,18,63,64]. The service temperature of such titanium alloys ranges from 4.2 K (Ti-5Al-2.5Sn) [6] to 1023 K (γ-TiAl, Ti-Nb-Mo) [5]. Moreover, equipment used to melt titanium alloys prior to casting are based on induction skull melting (ISM) [19,65], vacuum arc re-melting (VAR) [66], electron beam melting (EBM) [20,67] and vacuum induction melting (VIM) [23,24,68].

2.2. Procedure

Investment casting begins by producing patterns of a desired shape, which can then be connected into a tree assembly to cast multiple parts simultaneously. The pattern assembly is then coated in a ceramic slurry and rained with stucco sand. Stucco enhances mechanical bonding between the layers, and distributes local stresses during drying to minimize cracking [70,71]. The ceramic slurry comprises of a ceramic refractory, a binder, and ash or fibers to improve permeability and green body strength of the shell mold. The slurry-coating and stuccoing processes are repeated with intermittent drying between layers, until a desired thickness is obtained as is illustrated in Fig. 4. Care should be taken to ensure that the corners and edges are evenly coated and stuccoed as the flat regions, to prevent premature breaking under small loads [72–74].

A sealcoat is the final dip, after which no stucco is applied. Dip coating typically takes 30 s, then excess material is drained for about 1 h. The primary and sealcoat are dried for 24 h, while the intermediate secondary layers are dried for 1–5 h at an average air speed of 35 m s^{-1} [75]. The assembly is then dewaxed, commonly in an autoclave, and the remaining shell mold is sintered to increase its density, strength and modulus of rupture [56,57]. During the actual casting step, molten titanium is poured into the finished mold to cast the desired shape (see Fig. 3). Once the alloy solidifies, the ceramic shell mold is shattered, and the castings are cut from the tree assembly into individual castings. The castings are then ground, polished and surface treated as needed to finish. If the titanium part is for a biomedical implant, a surface roughness of less than 5 μm is vital for cell attachment and proliferation [63,76]. Therefore, post-casting processes such as electropolishing and heat treatment are performed to obtain the desired roughness and wear resistance of the surface [77–79].

2.3. Modeling in investment casting

There are two main forms of investment casting—gravity and centrifugal casting [69,80]. The traditional form is gravity investment casting, where the mold is stationary and gravity is the only force aiding to fill the mold cavity. A modern setup is centrifugal investment casting, where the mold rotates as the cavity is filled. Centrifugal casting was reported to be advantageous for very thin parts with complex shapes because it achieves higher castability, less cracks and less porosity than gravity investment casting [69,80–82]. Modeling of gravity and centrifugal investment casting is examined below.

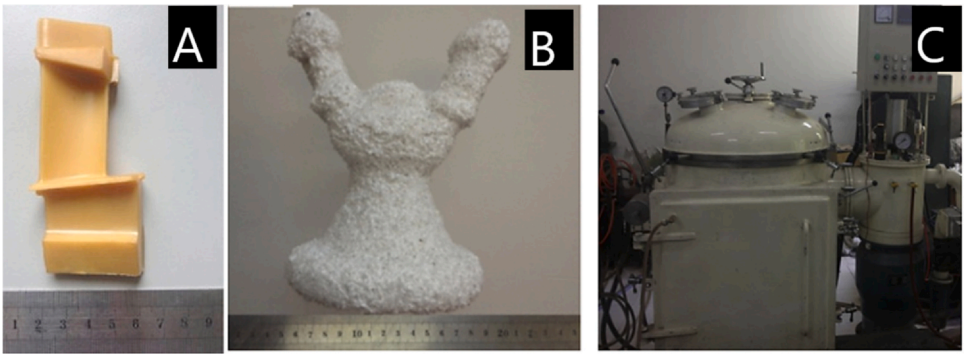

Fig. 3. Wax pattern (A), ZrO_2 ceramic mold (B), and a vacuum induction furnace used to melt a Nb-TiAl alloy for investment casting (reprinted with permission from Ref. [69]). These images highlight the main stages of an investment casting process—pattern-making, mold-making, and casting of the molten alloy.

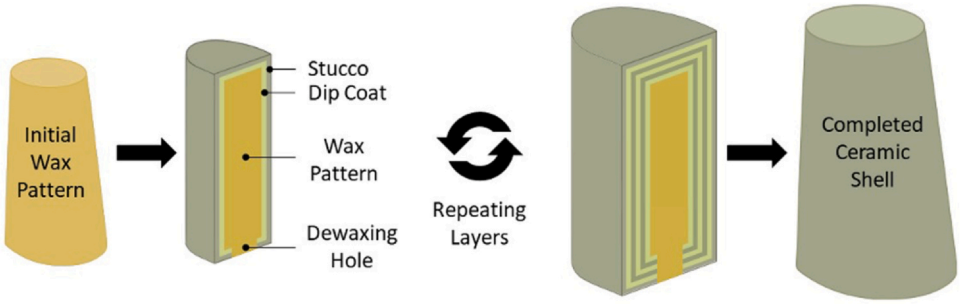

Fig. 4. Schematic illustration of the successive coating and stuccoing process to get a desired thickness of a ceramic shell mold (reprinted with permission from Ref. [74]).

2.3.1. Fluid flow

To get an expression of fluid flow, two recent models [69,80] can be combined to yield an amended expression. The molten metal is assumed to be an incompressible Newtonian fluid (constant density), whereas this simplification allows for conservation of momentum and application of the Navier-Stokes equation in relationship (1).

$$\rho\left(\frac{\partial\vec{v}}{\partial t}+\vec{v}\cdot\nabla\vec{v}\right)=-\nabla P+\rho g+\mu\nabla^2\vec{v} \tag{1}$$

$$\nabla\vec{v}=\left(\frac{\partial u}{\partial x}+\frac{\partial v}{\partial y}+\frac{\partial w}{\partial z}\right) \tag{2}$$

where ρ is density, $\vec{v}$ is velocity, t is time, P is pressure, g is gravitational acceleration, μ is dynamic viscosity of the liquid metal, and $\vec{v}$ is the velocity vector. Eq. (2) is a three-dimensional expression of the velocity vector in terms of (u, v, w), and directions (x, y, z) respectively. Overall, the left side of Eq. (1) represents fluid acceleration and convection, while the right side represents pressure gradient, external forces acting on the body, and viscosity effect on fluid velocity, respectively.

Simplifying further, conservation of mass with no source or sink gives Eq. (3). Moreover, since the metal is considered to have constant density, the mass conservation equation reduces to Eq. (4) which can also be expressed as continuity by Eq. (5) [69].

$$\frac{\partial\vec{v}}{\partial t}+\rho\nabla\vec{v}=0 \tag{3}$$

$$\nabla\vec{v}=0 \tag{4}$$

$$\frac{\partial u}{\partial x}+\frac{\partial v}{\partial y}+\frac{\partial w}{\partial z}=0 \tag{5}$$

In centrifugal investment casting specifically, the velocity of the alloy melt as the equipment rotates can be solved by Eq. (6) [80].

$$\vec{v}_r=\vec{v}-(\vec{\omega}\times\vec{r}) \tag{6}$$

Where, r is the position vector, $\vec{v}_r$ is the relative velocity and ω is the angular velocity. Therefore, a relationship for modeling fluid flow (momentum transfer) in centrifugal investment casting can be obtained by substituting Eq. (6) into Eq. (4) which results in expression (7).

$$\frac{\partial\vec{v}_r}{\partial t}+\rho\nabla\vec{v}_r=0 \tag{7}$$

2.3.2. Solidification

To model the solidification of a TiAl alloy during investment casting, the previously analyzed models can be applied to develop an expression for heat transfer through the ceramic shell as shown in Eq. (8) [69,80].

$$\rho C_p\left(\frac{\partial T}{\partial t}+\vec{v}\cdot\nabla T\right)=k\nabla^2T+L\frac{\partial f_s}{\partial t} \tag{8}$$

where, C_p is the specific heat capacity, k is the thermal conductivity, T is the temperature, L is the latent heat, and f_s is the fraction of the solid phase.

So far, expressions for modeling momentum and heat transfer involved in centrifugal and gravity investment casting, particularly for TiAl and Nb-TiAl alloys, have been presented. Experimental validation confirmed that these models predicted bubble formation during turbulent flow, which causes porosity [80]. Additionally, it was observed that centrifugal investment casting led to less thermal stress cracks than gravity investment casting, as is shown in Fig. 5 [69]. Nonetheless, the faster cooling rate in centrifugal investment casting caused γ-phase segregation on the edges of the Nb-TiAl

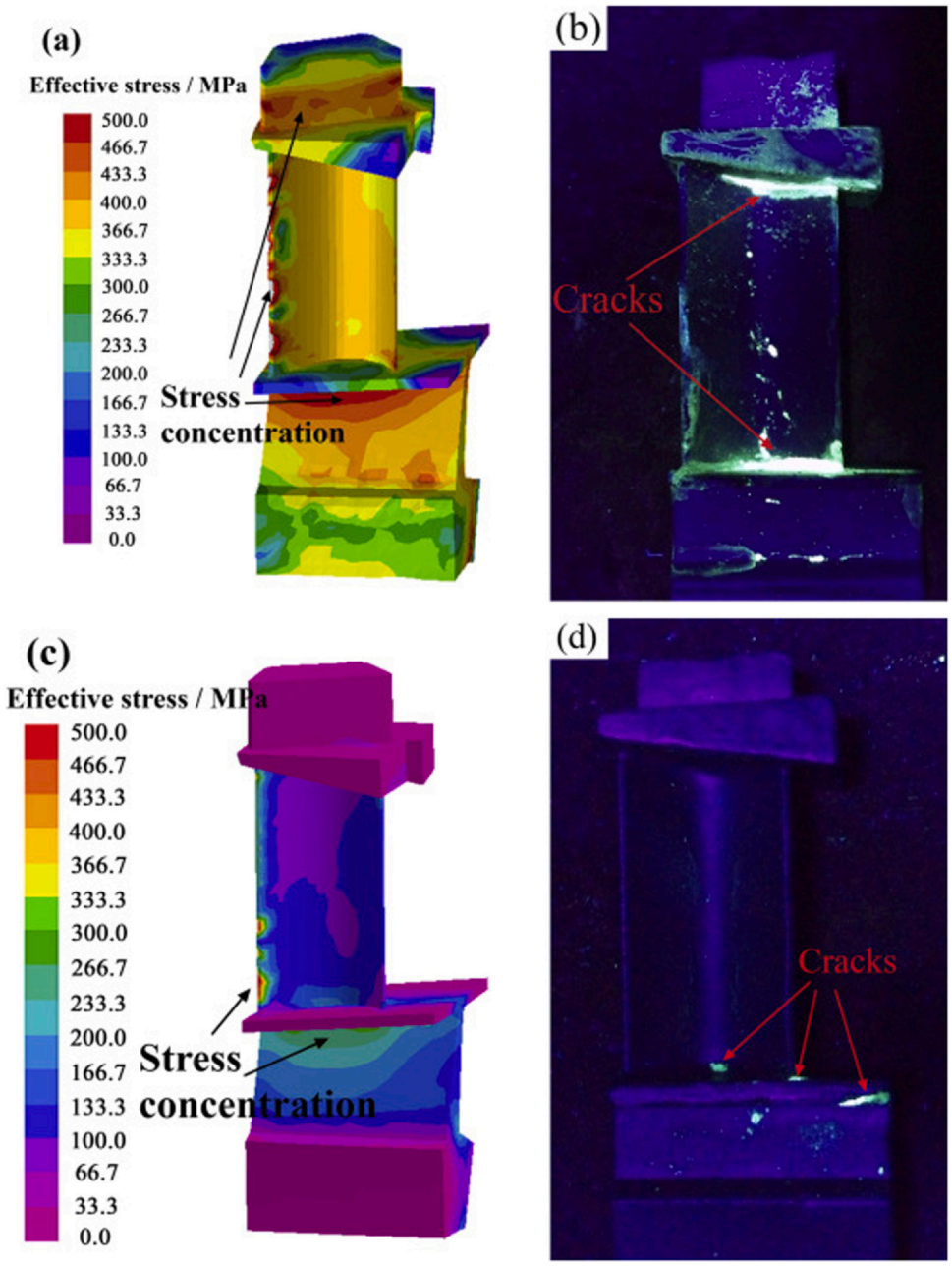

Fig. 5. Model simulations and corresponding experimental validation showing higher stress cracks in the gravity investment casting than in the centrifugal investment casting. (a, c) are models while (b, d) are florescent images of actual cast Nb-TiAl blades (reprinted with permission from Ref. [69]).

castings, which was absent on those cast using the gravity investment method [69].

2.3.3. Mass transfer

Oxide ceramic refractories generally have a higher corrosion resistance in contact with titanium alloys than carbide, nitride and boride ceramics [22,25,84,85]. Furthermore, many oxide ceramics have an exceptional creep resistance even at temperatures close to 2000 °C [84]. Therefore, they are preferred for investment casting molds. Nevertheless, mass transfer of oxygen from oxide shell molds during casting remains an important concern. Conventional titanium sponge produced by the Kroll process contains oxygen in a solid solution in the range of 0.02–0.04 wt%, which is considered the lower limit for this processing method [86–88]. Nevertheless, commercial titanium alloys generally contain 0.1–0.4 wt% oxygen to increase the strength [88,89]. Currently, researchers continue to research corrosion-resistant refractories and high temperature processing methods to minimize unwanted mass transfer of contaminants like oxygen exceeding this limit during melting and casting.

Modeling techniques are a modern approach to understand, predict and optimize the corrosion resistance of ceramic shell molds in contact with titanium alloys during casting. For example, the model presented in Eq. (18), successfully predicted the α-case thickness during the casting of Ti-6Al-4V in zirconia shell molds. It was found that the amount of diffused oxygen at the surface of the casting ranged from 5 to 9.5 wt%, while that at the limit of the α-case region the oxygen content was only 0.02 wt% higher than in the bulk of the alloy [33]. These experimental results agreed well with thermodynamic calculations for β-Ti in contact with ZrO_2. It can be seen

that tracking the diffusion of oxygen into the titanium β phase is an effective route in modeling mass transfer during the formation of α-case on β and ($\alpha+\beta$) titanium alloys [33,34]. This is because α-case formation is a high temperature phenomenon that occurs when a titanium alloy that is above its β transus temperature (thus at a 100% fraction of the β phase), is cooled to ambient temperature after oxidation [34]. For a Ti-6Al-4V alloy, the β transus is around 937 °C (≈1210 K), but the strong α-stabilizing effect of oxygen increases the β transus temperature as a function of the oxygen content, as is approximated by Eq. (9) [90]. Due to the oxygen diffusion, the surface becomes significantly richer in α phase as indicated in Fig. 7, altering the microstructure and properties compared to the bulk.

$$1210\text{K} + 242.7\text{K}\cdot\text{wt\%O}_2 \tag{9}$$

A simple model to predict the α-case thickness developing during investment casting of a Ti-6Al-4V alloy in a zirconia shell mold is described below [33]. Assumptions taken into account to solve this mass transfer problem are as follows:

- One-dimensional, thin planar surface (negligible temperature changes over the α-case thickness)
- Diffusion coefficient D changes with time t and is expressed as $\tau = Dt$
- Isothermal diffusion, i.e. constant diffusion coefficients and constant boundary concentrations (C_0 and C_∞). Here, C_0 is the oxygen concentration at the metal-mold interface and C_∞ is the oxygen concentration in the bulk alloy.

The concentration at the surface is at the beginning identical to the one in the bulk material, i.e. the initial condition (*I. C.*):

$$C(x, t=0) = C_\infty \tag{10}$$

The boundary conditions (*B. C.*) are accordingly defined:

$$C(x=0, t) = C_0 \tag{11}$$

$$C(x=\infty, t) = C_\infty \tag{12}$$

where $x=0$ is the outer surface of the metal and $x=\infty$ is the bulk alloy.

The concentration profile of oxygen at position x into the alloy after a given time t is given by Fick's second law of diffusion, given in Eq. (13). Applying the initial and boundary conditions, the concentration profile can then be solved by Eq. (14).

$$\frac{\partial C}{\partial t} = \frac{\partial}{\partial x}\left(D\frac{\partial C}{\partial x}\right) \tag{13}$$

$$C = C_0 - (C_0 - C_\infty)\,\mathrm{erf}\left(\frac{x}{\sqrt{4Dt}}\right) \tag{14}$$

The α-case layer, however, grows as a function of time and temperature. Therefore, the product Dt can be scaled to include both factors.

$$\tau = \int_0^t D(T(t'))\mathrm{d}t' = D(T(t)) \tag{15}$$

Here, D changes with time and temperature, while the concentrations (C_0 and C_∞) are still taken to remain constant given a small α-case layer. The solution in Eq. (14) remains valid even when the product Dt is replaced by the scaled time τ.

The diffusion coefficient depends on the temperature T, the activation energy Q, the gas constant R and the frequency factor D_0 (Eq. (16)), which can be substituted into the equation for the scaled time (Eq. (15)), resulting in Eq. (17). The frequency factor D_0 can be assumed as the reference diffusion coefficient at solidus temperature [91].

$$D = D_0 \exp\left(-\frac{Q}{RT}\right) \tag{16}$$

$$\tau = D_0 \int_0^t \exp\left(-\frac{Q}{RT(t')}\right)\mathrm{d}t' \tag{17}$$

The goal of the calculation is to model the penetration depth of oxygen $x^*(t)$ in the titanium casting, whereas C^* is the oxygen concentration at the limit of the α-case. Generally, C^* can be obtained by electron microscopy and is only slightly higher than the oxygen concentration in the bulk material. Hence, substituting Eq. (17) in Eq. (14), gives the solution in Eq. (18).

$$x^*(t) = 2\lambda\sqrt{\tau} \tag{18}$$

where λ is the solution of the following equation:

$$\mathrm{erf}(\lambda) + \left(\frac{C^* - C_\infty}{C_0 - C_\infty}\right) - 1 = 0 \tag{19}$$

Parameters that govern the final thickness of an α-case layer after solidification are therefore the starting temperature or time in the integration, the activation energy Q, and the product $\lambda\sqrt{D_0}$ which is directly proportional to the final α-case thickness. To obtain a numerical solution, specific alloy and mold material values can be entered in the model. For example, examining Ti-6Al-4V cast in a mold with a ZrO_2 facecoat, the best results for the simulations were achieved for a temperature of 1875 K (7 K higher than the solidus temperature), $D_0 = 51.2\ \mathrm{cm^2\ s^{-1}}$, $\lambda = 2.13$ and $Q = 249$ kJ/mol [33]. The model presented was later applied in other studies that also coupled impurity diffusion to microstructure evolution and mechanical properties [92–94].

3. Effect of mass transfer on microstructure and properties

Pure titanium has three main microstructure phases—β at high temperatures (above 1156 K), ω at cryogenic temperatures, and α in between [97]. Pressure changes can also cause phase transformations, for example, at room temperature α transforms to ω at ≈ 9 GPa [97]. Nonetheless, alloying elements can be used to stabilize even metastable ω and β phases at ambient temperature [98]. Stabilizers of the β phase include vanadium, niobium, molybdenum and nickel, while α phase stabilizers include oxygen, carbon, nitrogen and aluminum [8,99]. Notably, oxygen levels of at least 4.8 at% stabilized both the α and ω phases in a β type Ti-20Nb alloy [100]. However, a martensitic transformation from α to ω can drastically decrease the ductility of Ti-6Al-4V and titanium A-70 alloys, but presence of O, Al, N, or C aided in suppressing this transformation by increasing the energy barrier [97]. For instance, such impurity/alloying elements, especially O and Al, increased the estimated transformation pressure of Ti-6Al-4V from 13 to 63 GPa [97]. Contrarily, vanadium favored the α to ω transformation by decreasing the energy barrier. Understanding the role of impurity elements in phase stability is therefore vital for alloy design and application.

Alpha-titanium has a hexagonal close packed (hcp) structure and can dissolve over 30 at% oxygen in solid solution, as displayed in the Ti-O phase diagram given in Fig. 6 [83]. On the other hand, β-Ti has a body centered cubic (bcc) structure and a much lower oxygen solubility of only 2 at% at 1273 K, which increases at higher temperatures [101]. As evident from Fig. 6, the α to β transition temperature is directly affected by the oxygen content. The higher the oxygen content, the higher the transition temperature, because oxygen stabilizes the α phase region [101,102]. Overall, oxidation of titanium at elevated temperatures above 750 K, occurs in two simultaneous steps—(i) formation of a thin oxide scale on the surface, and (ii) inward diffusion of O_2 into the bulk forming an oxygen-rich layer or α-case beneath the scale [37,99].

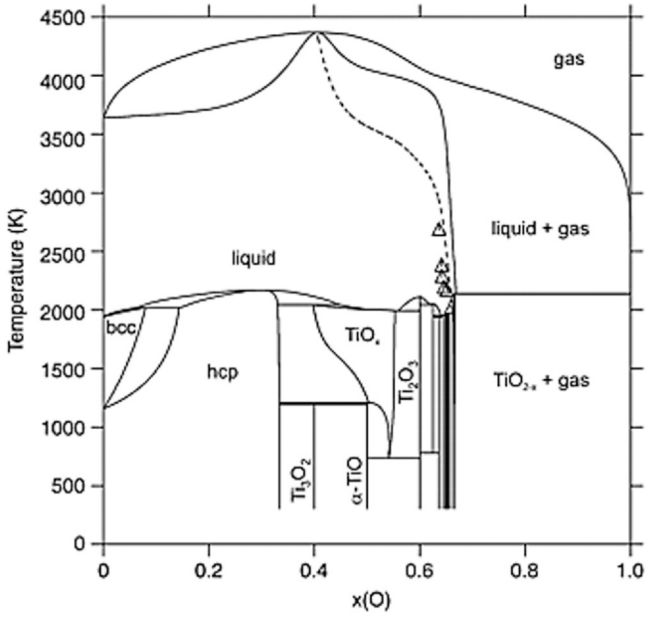

Fig. 6. Ti-O phase diagram showing complete solubility of oxygen into titanium up to 32 at%, before forming an oxide (reprinted with permission from Ref. [83]). The entire composition range is evaluated at a total pressure of 0.1 MPa, while the dashed lines represent experimental data at an oxygen partial pressure P_{O_2} of 13.33 Pa.

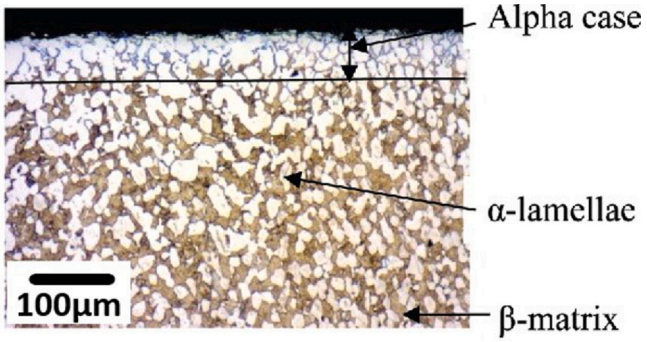

Fig. 7. Optical image of Ti-6Al-4V showing the α/β microstructure, and an α-case layer that developed when the alloy was annealed at 930 °C in air for 1 h (reprinted with permission from Ref. [50]).

Mass transfer of oxygen into titanium alloys directly affects their microstructure as demonstrated in Fig. 8. Consequently, the mechanical properties are also altered, as summarized in Table 1. It can be seen that the alloy strength increases with an increasing oxygen content, whereas the ductility and fracture toughness decrease. Interestingly, after investment casting of cp-Ti in an alumina mold, TEM and EDS examinations (Fig. 9) of the α-case layer showed not only presence of oxygen but also aluminum [32,103]. Moreover, other studies also show that the α-case layer on titanium alloy castings comprises of sub-layers which include a reaction layer and a hardened diffusion layer [27,31,32,93]. Such a layered microstructure is displayed in Fig. 10.

3.1. Hardness and wear resistance

Hardness can be defined as a material's resistance to indentation or abrasion, and wear as the degree to which the material abrades. Wear resistance typically increases with increasing hardness. It is known that as-machined or as-cast titanium alloys have poor wear resistance [8,15], but heat treatment and surface modifications greatly enhance their wear resistance [39,41,104]. Heat treatments work by altering the alloy microstructure which in turn changes its mechanical properties. For example, compared to cold-rolled Ti-13Nb-13Zr and Ti-6Al-4V solution-treated in the $\alpha+\beta$ region, it was found that the Ti-6Al-4V which was solution-treated above the β transus temperature and subsequently water-quenched, had superior wear resistance than the former two alloys [104]. This difference was due to formation of a hard martensitic microstructure in the latter Ti-6Al-4V alloy. Other than heat treatments, coatings of hard ceramic materials like TiC and TiN are also common for specifically enhancing wear resistance of titanium alloys [15].

In investment casting, metal-mold reactions and subsequent formation of the α-case layer on titanium alloys substantially increase surface hardness as shown in Fig. 10 [32]. Thickness of the α-case layer typically increases parabolically, meaning that it grows rapidly at the beginning and then slowly at prolonged exposure time and temperature [37,45]. Thus, it is not surprising that the activation energies for parabolic oxidation and α-case formation are very close, for example, 157 kJ/mol and 153 kJ/mol, respectively for Ti-6Al-2Sn-4Zr-2Mo (Ti-6242) alloy [37]. Nonetheless, a transition in oxidation kinetics from parabolic to linear was observed when wrought Ti-6242 alloy was heat-treated at 700 °C in air for more than 200 h [37].

The hardness of titanium alloy castings can be controlled by adjusting the mold preheat temperature, mold composition, and casting thickness. Preheating the mold is especially beneficial for limiting thermal shock in the ceramic shell mold and to ensure complete mold filling [74,105]. As displayed in Fig. 11(a), increasing the preheat temperature of the shell mold from 400 °C to 600 °C led to a substantial increase by about 100 HV in the surface hardness of the Ti-6Al-4V castings [29]. Strikingly, there was negligible difference in surface hardness of Ti-6Al-4V cast in a calcium zirconate mold either at room temperature or preheated to 400 °C [29]. Moreover, as seen in Fig. 11(b), an increase in hardness was also observed for thicker parts which can be inferred from the slower solidification.

A trend of hardness increasing with a higher preheat temperature and part thickness was also reported for Ti-46Al cast in molds with an alumina facecoat [26]. Molds in which the bulk material is distinct from the facecoat material can be termed as composites. The surface material—the facecoat—typically has higher corrosion-resistance, but is significantly more expensive than the underlying bulk materials [26,106,107]. However, in several studies that applied composite molds, for example alumina-coated silica, bulk elements diffused from the bulk material through the facecoat and into the titanium alloy casting [26]. As noted previously, surface hardness is not only affected by diffused oxygen, but also by metallic elements from the mold including aluminum and silicon [32,93,94]. Hence, further studies are needed to optimize composite investment molds to limit bulk material diffusion, but also to reduce their overall cost.

3.2. Fracture toughness and tensile strength

Fracture toughness is the ability of a material to resist further crack growth, and is a crucial property to ensure safety under service conditions. Under simple uniaxial loading, the critical stress at the crack tip necessary to cause catastrophic failure can be calculated using Eq. (20). The α-case layer that develops on titanium alloys during high temperature processing is brittle, and under tensile loading micro-cracks were observed to nucleate and propagate from this layer as revealed in Fig. 12 [45,92]. Interestingly, surface crack initiation time can be calculated based on the α-case thickness as is shown in Eq. (22) and Fig. 12(b). Examination of this brittle α-case layer was performed on titanium IMI834 (Timetal 834), exposed to creep conditions at up to 923 K and 140 MPa [45].

$$K_{Ic} = Y\sigma\sqrt{\pi c} \tag{20}$$

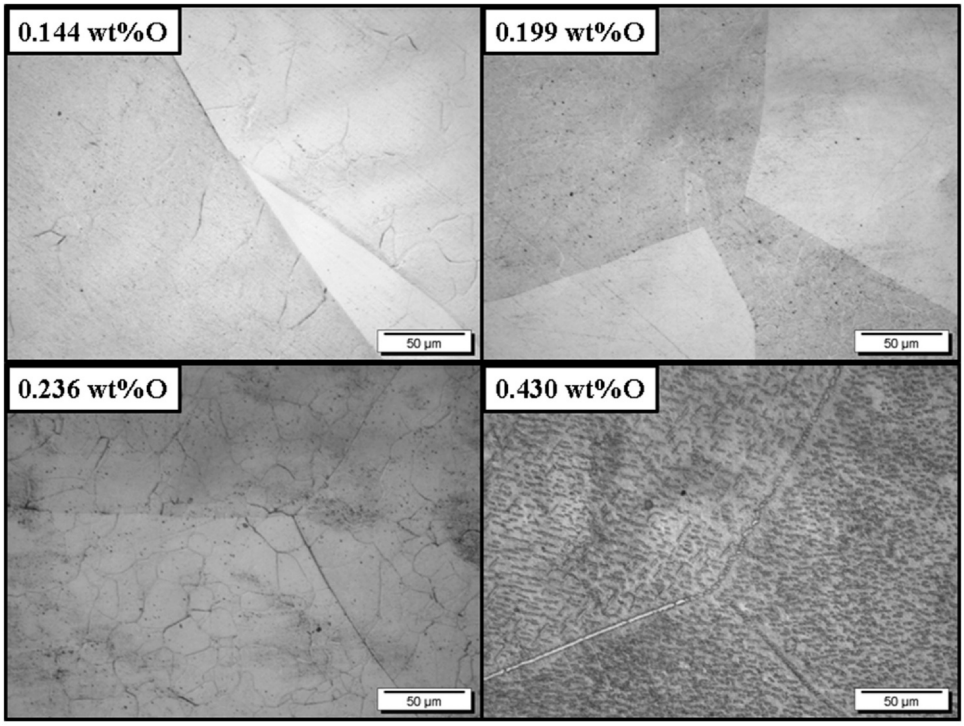

Fig. 8. Influence of oxygen diffusion on the microstructure of the β titanium alloy Ti-15Zr-7.5Mo. The large beta grains were permeated by a needle-shaped orthorhombic α'' phase as the oxygen content increased. This microstructure change led to a subsequent increase in hardness (reprinted with permission from Ref. [96]).

$$c = \frac{1}{\pi}\left(\frac{K_{Ic}}{\sigma Y}\right)^2 \tag{21}$$

where c is the crack length, K_{Ic} is the fracture toughness, Y is a geometric factor, and σ is the applied engineering stress.

$$t_{crack} = t_f - t_\alpha \tag{22}$$

where t_{crack} is the initiation time for a surface crack to form, t_f is the total time to fracture (under tension), and t_α is the time required for an α-case layer of a given thickness to develop on each titanium IMI834 specimen. Overall, samples that had a thicker α-case layer cracked earlier under lower stresses and lower strains, than samples that had a thin or negligible α-case.

Any contamination during melting and casting affects the properties of the final cast part, so it is imperative to examine interfacial mass transfer from crucibles and molds. Titanium alloys are typically molten in water-cooled copper crucibles, but several studies investigated the use of ceramic crucibles for improved energy efficiency and a higher melting volume [21–24]. In a study examining the effect of crucible materials on properties of Ti-46Al castings, the alloy molten in a yttria crucible had a higher tensile strength and a comparable fracture toughness to that molten in a water-cooled copper crucible, as shown in Fig. 13 [22]. Interestingly, a considerable reduction in mechanical properties of Ti-46Al castings was only observed above 0.5 wt% dissolved oxygen as demonstrated in Fig. 14(a) [22].

Upon cooling, especially yttria precipitates from the alloy melt and mostly coalesces along grain boundaries. Micro-cracks are observed to form around such precipitates as demonstrated in Fig. 15 [108].

It is suggested that the conventional threshold of utmost 0.1 wt% oxygen for TiAl alloys could be revised because empirical results showed that significant reduction in mechanical properties occurs at higher levels than this limit [22]. Increasing the upper limit of permissible dissolved oxygen could reduce the cost of titanium alloys and expand their applications to the automotive industry as recently proposed [82,109]. On the other hand, it is notable that a drastic decrease in tensile strength can occur when more than 1.0 wt% of metallic elements, particularly from Y_2O_3 and ZrO_2, are dissolved in Ti-46Al castings (see Fig. 14(b)) [22].

3.3. Fatigue life and Young's modulus

Load-bearing titanium parts are frequently subjected to cyclic stresses which can accumulate plastic deformation making the part susceptible to fatigue cracking [44,110]. Notably, fatigue life is inversely proportional to Young's modulus, where Young's modulus refers to a material's stiffness or resistance to elastic deformation. A dilemma is presented, however, because titanium alloys for hard tissue implants with a lower Young's modulus are more compatible with bone, but they also often have poor fatigue resistance [10,110]. The most traditionally used Ti-alloys—cp-Ti and Ti-6Al-4V ELI—have

Table 1
Effect of oxygen content and microstructure on the mechanical properties of Ti-6Al-4V [8,95]. Yield strength (YS), ultimate tensile strength (UTS), elongation (EL), reduction in area (RA), and fracture toughness (K_{Ic}), respectively.

O_2 (wt%), microstructure	YS (MPa)	UTS (MPa)	EL (%)	RA (%)	K_{Ic} (MPa$\sqrt{m}$)
0.18–0.2%, equiaxed	1068	1096	15	40	54
0.15–0.2%, equiaxed	951	1020	15	35	61
0.15–0.2%, lamellar	884	949	13	23	78
Max. 0.13%, equiaxed	830	903	17	44	91

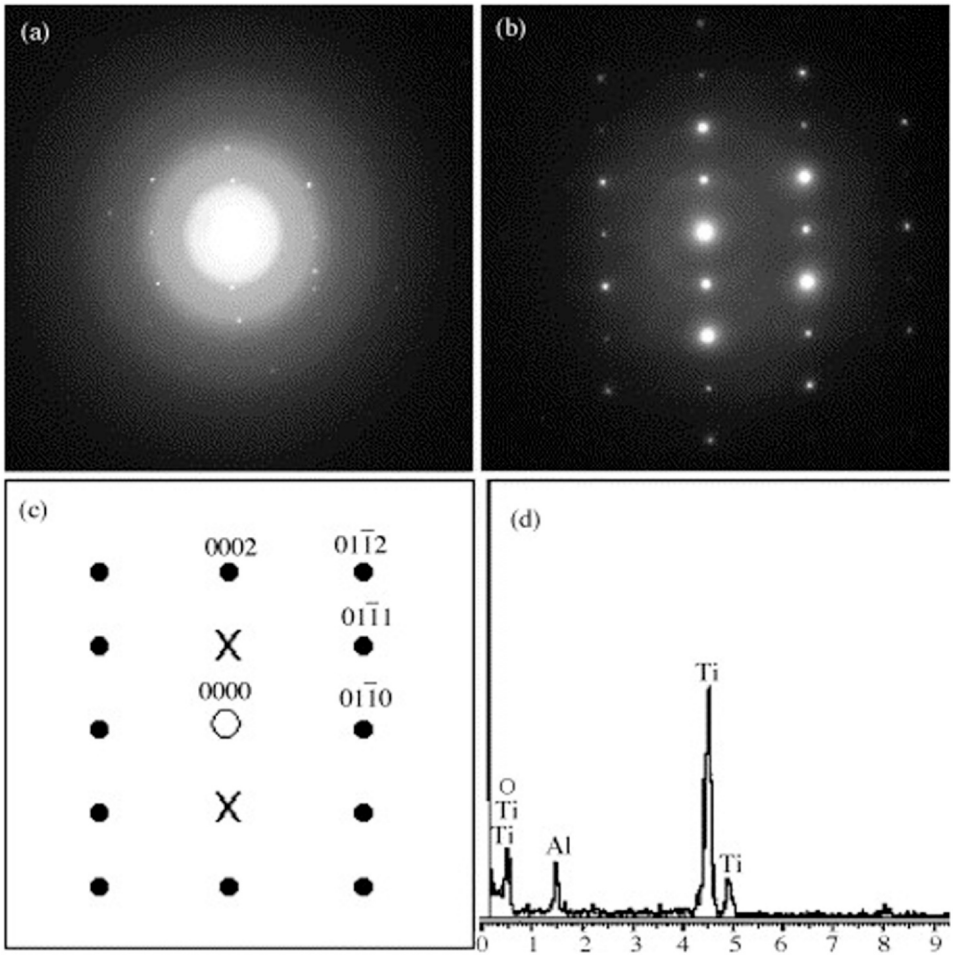

Fig. 9. TEM and EDS analysis of a cp-Ti casting showing crystallography and elements in the α-case layer; (a) ring and spot patterns; (b) spot diffraction; (c) indexed pattern of the hcp phase; (d) EDS histogram showing both interstitial oxygen and substitutional aluminum in the α-case layer (reprinted with permission from Ref. [32]).

Young's moduli of 108 GPa, and up to 118 GPa respectively, depending on the processing method [111–113]. Contrarily, the Young's modulus of human bone ranges between 10 and 30 GPa [7,114]. Therefore, substantial materials engineering led to development of a new titanium Ti-29Nb-13Ta-4.6Zr (wt%; TNTZ) alloy, which has a lower Young's modulus than cp-Ti and Ti-6Al-4V [115,116]. Furthermore, unlike Ti-6Al-4V which was reported to cause toxicity side effects in the body due to presence of vanadium and aluminum [12,13], TNTZ is free from these potentially harmful elements [115].

Optimization of the counteracting properties of fatigue life and Young's modulus is a challenge, and different processing techniques are employed including cold rolling, and heat treatments like α and ω phase precipitation hardening [110,112,116,117]. Recently, enhanced fatigue life and exceptionally low Young's modulus (40 GPa), were observed in near-β Ti-22Nb-6Zr alloy by inducing a polygonized nano-subgrained dislocation microstructure [110]. The nano-subgrained structure was obtained after post-deformation annealing at 600 °C for 0.5 h, where this alloy portrayed a reversible stress-induced β to α" phase transformation at high strains (0.3%) [110]. These features enabled superlasticity and superior fatigue resistance compared to the strain-hardened and recrystallized counterparts.

Interestingly, it was found that diffusion of up to 70 wt% oxygen into a β-type TNTZ alloy improved its fatigue life to 650 MPa, while maintaining a low Young's modulus of 76 GPa [10]. The high concentration of oxygen improved fatigue life of the TNTZ alloy by facilitating formation of cohesive slip planes, and small, densely-arranged martensitic α" twins [10]. Contrarily, mass transfer of oxygen leading to an α-layer of 2 μm decreased the low cycle fatigue life of Ti-6Al-2Sn-4Zr-2Mo (wt%; Ti-6242) specimens by 50%, and by 90% when the α-case thickness was 10 μm [44]. Comparably, in cp-Ti, Ti-6Al-4V, and Ti-15Zr alloys, microhardness and Young's modulus changed linearly with increasing oxygen content, which can be especially attributed to solid solution strengthening arising from interstitial oxygen atoms in the crystal structure of the alloy [10,39,45,118]. Conversely, for Ti-15Zr-xMo (x = 5, 7.5, 10, 15, 20 wt%), a non-linear dependence of the microhardness and Young's modulus on the oxygen content was reported, which was associated with a pinning effect of the interstitial elements in the metallic matrix [96]. Therefore, the effects of oxygen diffusion on the resulting mechanical properties vary with the titanium alloy type.

3.4. Biocompatibility

Investment casting of titanium implants leaves an α-case layer on the surface of the castings because of metal-mold reactions [31,92,93]. On the other hand, when oxygen diffusion is controlled, often through a heat treatment, an oxygen-rich surface layer is formed on titanium which mitigates wear and bio-corrosion [41,119,120]. In vivo studies of medical implants have identified four different types of corrosion including galvanic, pitting, crevice, and fretting corrosion, whereas different parts of implants experience

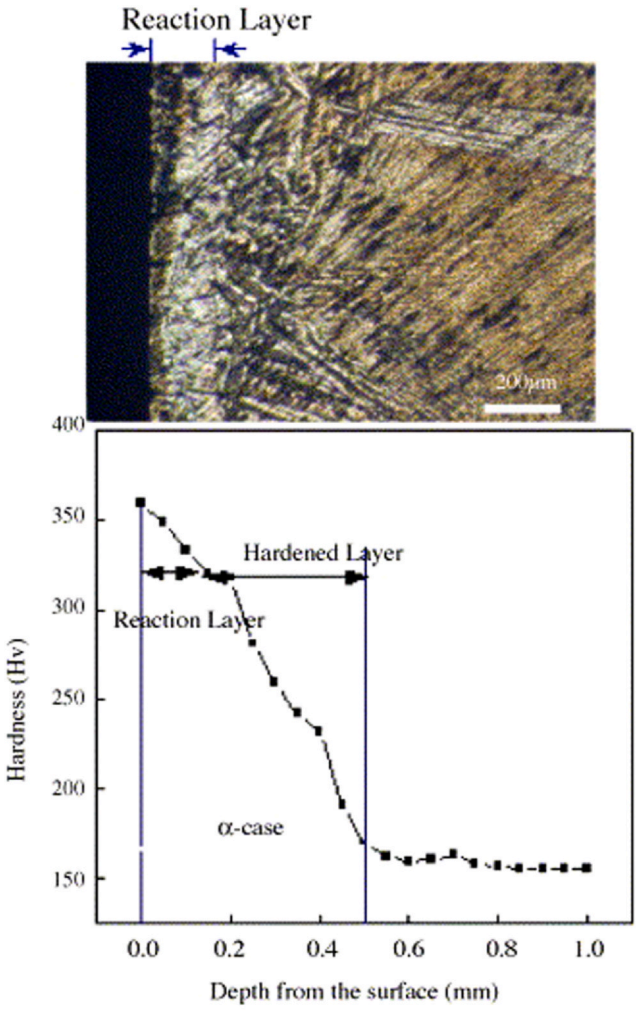

Fig. 10. Optical micrograph of a cp-Ti casting showing the sublayers that make up the α-case. The surface hardness is drastically different from the bulk alloy (reprinted with permission from Ref. [32]).

these types of corrosion to a varying degree. For example, attachment sites such as a screw or the femoral head of an artificial hip are more likely to experience wear due to crevice corrosion [9,121], while bearing surfaces such as the stem of an artificial hip is more likely to experience pitting and fretting corrosion [121]. Notably, galvanic corrosion was reported when two different metals sheared against each other in the implant, even if the oxide layer was present. Most recent cases of this interaction were reported for titanium and gold [9]. Corrosion is also increased with the introduction of fluoride to a dental implant [122]. These instances of corrosion eventually result in immune responses and implant failure [9].

Secondly, a study testing the thickness of the oxidation layer in relation to corrosion resistance showed that in comparison to a natural oxide layer at room temperature (≈5–10 nm [37,99]) a 100 nm thick oxidation surface layers enhanced the corrosion resistance of the implant [119]. Although there is not yet an absolute solution to wear due to corrosive fluids in the body [9,123], wear resistance of implants can be also improved by surface treatments and coatings. For example, orthopedic implants are often treated with calcium phosphate and bisphophonates coatings to improve biocompatibility by stimulating osteoconduction and bone resorption, respectively [121,124,125]. It should be noted that a discontinuous or very thin α-case layer on joint implants can break down and release wear debris from the surface of the implant [126,127]. When the wear debris is absorbed by the surrounding tissues, this triggers a foreign body inflammatory response and osteolysis in areas surrounding the implant. These responses often cause loosening of the implant, and at worst bone loss [126,128]. Overall, surface case hardening of titanium biomedical alloys through oxygen diffusion could be beneficial if performed in a controlled atmosphere [39,41].

4. Mitigation of mass transfer

Current solutions to address the problem of mass transfer that occurs during investment casting of titanium alloys can be divided into three categories: (i) using specialized furnaces with a controlled melting atmosphere, (ii) using advanced crucible/mold materials, and (iii) machining or chemical pickling as post-casting processing steps.

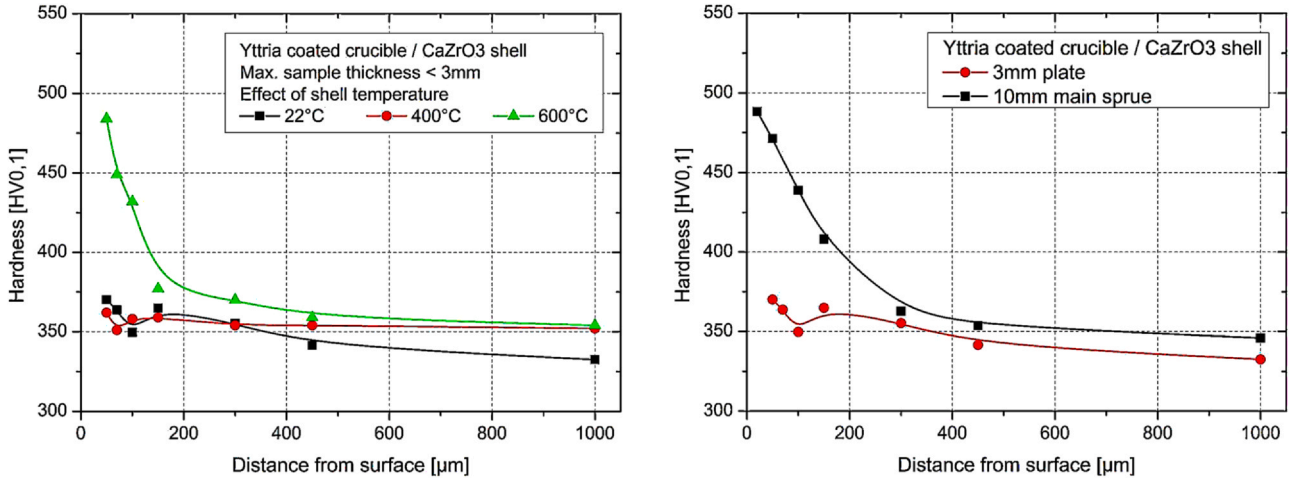

(a) Effect of mold preheat temperature (b) Effect of casting thickness

Fig. 11. Surface hardness of the castings increased with a higher preheating temperature and part thickness during investment casting of Ti-6Al-4V. However, there was a negligible difference in the hardness of castings produced with a $CaZrO_3$ mold at ambient temperature or one that was preheated to 400 °C (reprinted with permission from Ref. [29]).

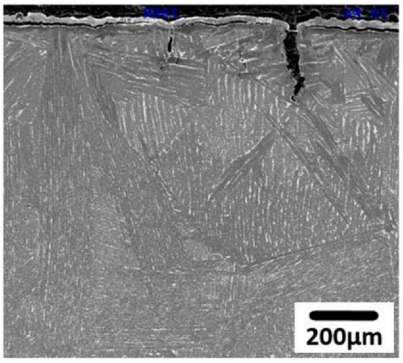

(a) Effect of oxygen mass transfer at the surface of a cp-Ti tensile specimen.

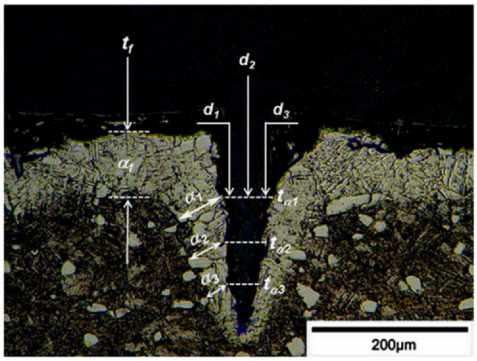

(b) Examination of the α-case layer on a crept titanium IMI834 specimen after creep testing.

Fig. 12. Cp-Ti tensile specimen with micro-cracks which nucleated and propagated from the hard and brittle α-case layer (a), and (b) prediction of crack initiation time, t_{crack}, based on the crack depths, d_{1-3}, that penetrated through varying α-case thicknesses, α_{1-3}, on a titanium IMI834 creep specimen ((a): reprinted with permission from Ref. [92], (b): reprinted with permission from Ref. [45]).

4.1. Melting techniques

Furnaces for melting titanium alloys typically have water-cooled copper crucibles in order to prevent potential interfacial diffusion associated with ceramic crucibles. These melting techniques include induction skull melting (ISM) [19,65], vacuum arc re-melting (VAR) [66], and electron beam melting (EBM) [20,67]. Such equipment is specifically made for alloys that are very reactive in molten state. However, these techniques are exceedingly energy intensive, accommodate only a small metal volume and are only able to achieve a low superheating temperature [65]. However, due to the commonly low fluidity of titanium alloys, a high superheating temperature is important to maintain a metal feed reservoir which minimizes cavities and porosity in the casting. For example, when using ISM, a superheating temperature of up to 62 K was measured, while the heating power was 350 kW for 4.5 kg of TiAl [65]. Contrarily, in another study that used vacuum induction melting (VIM)—a technique that uses ceramic crucibles—7 kg of a similar TiAl alloy was molten at only 20–35 kW [67]. Thus, VIM in a highly corrosion-resistant ceramic crucible is significantly more energy-efficient with additional potential benefits of a higher superheating temperature and the capability for larger castings than techniques that use water-cooled copper crucibles [23,24,68].

4.2. Crucible and mold materials

4.2.1. Alumina

Alumina investment molds have demonstrated relatively low reactivity with TiAl alloys with more than 30–40 at% aluminum [32,105,129]. From the titanium-aluminum phase diagram, it is known that an increasing aluminum content lowers the melting temperature of the alloy. For instance, the melting temperature of γ-TiAl is about 1460 °C while that of pure titanium is about 1670 °C [130]. Thus, titanium aluminide castings with a high aluminum content demonstrate a lower melting temperature and in contact with alumina molds less metal-mold reactivity and lower surface hardness than their counterparts (see Fig. 16) [32]. Furthermore, the presence of aluminum in both the alloy and the mold can promote interfacial kinetic stability by lowering the concentration gradient of aluminum. On the other hand, some studies have investigated

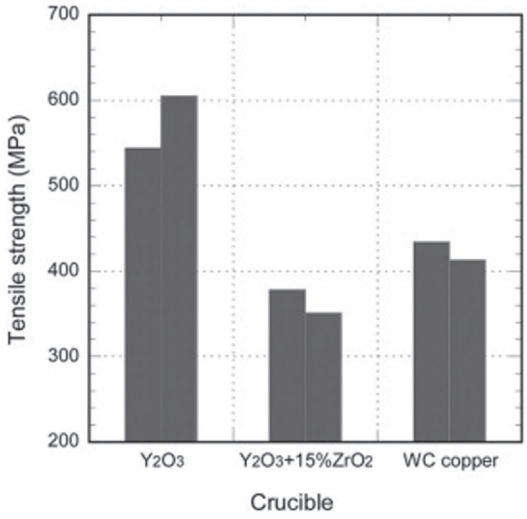

(a) Tensile strength of Ti-46Al molten in a water-cooled copper crucible versus ceramic crucibles

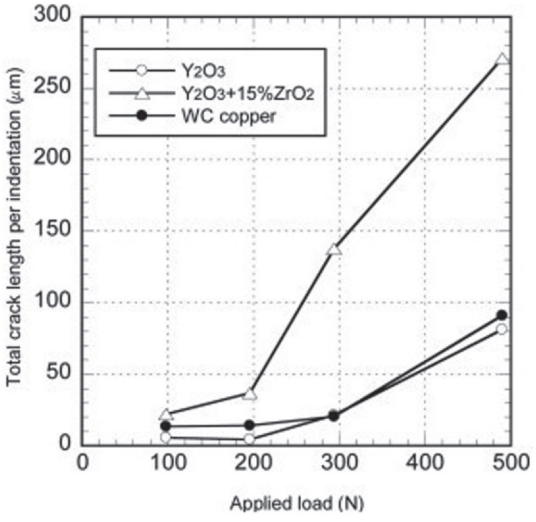

(b) Fracture toughness of Ti-46Al molten in a water-cooled copper crucible versus ceramic crucibles

Fig. 13. Comparing the effect of interfacial mass transfer from metallic versus ceramic crucibles on the tensile strength and fracture toughness of Ti-46Al. The specimen molten in the yttria (Y_2O_3) crucible had a higher tensile strength than the one molten in a water-cooled copper crucible (a), but the two had a comparable fracture toughness (b). Contrarily, Ti-46Al molten in the crucible made of zirconia had the least tensile strength and fracture toughness (reprinted with permission from Ref. [22]).

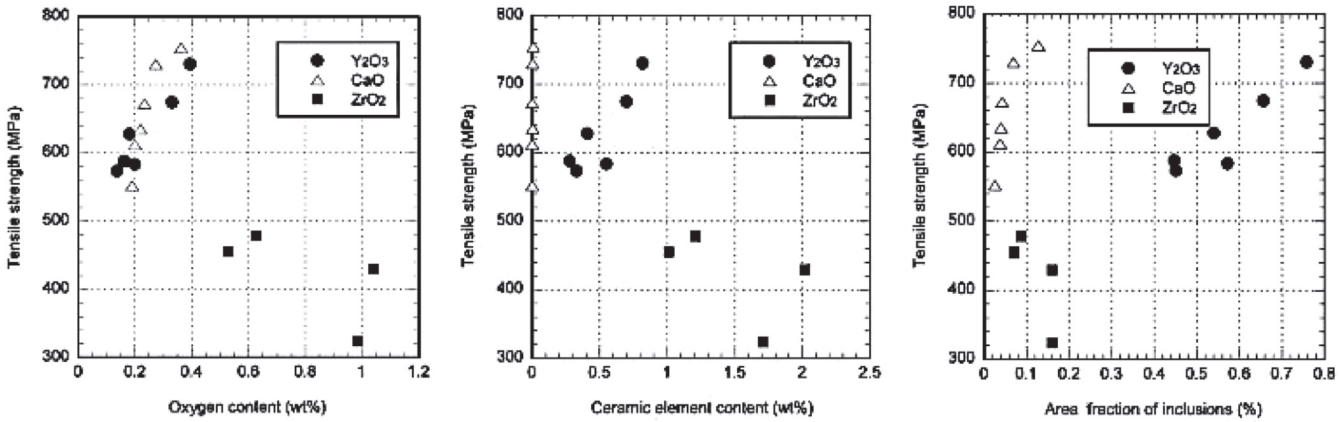

(a) Relationship between oxygen concentration and tensile strength

(b) Effect of metallic cation diffusion from ceramic molds on tensile strength

(c) Impact of area fraction of inclusions on tensile strength

Fig. 14. Mass transfer effect of oxygen and metallic elements from ceramic molds as well as ceramic inclusions on room temperature tensile strength of Ti-46Al castings. Tensile strength significantly decreased starting at 0.5 wt% oxygen and 1.0 wt% metallic impurities from the ceramic molds, respectively. Notably, the TiAl specimen molten in SiO_2 and Al_2O_3 crucibles were too brittle to be tested for tensile strength (reprinted with permission from Ref. [22]).

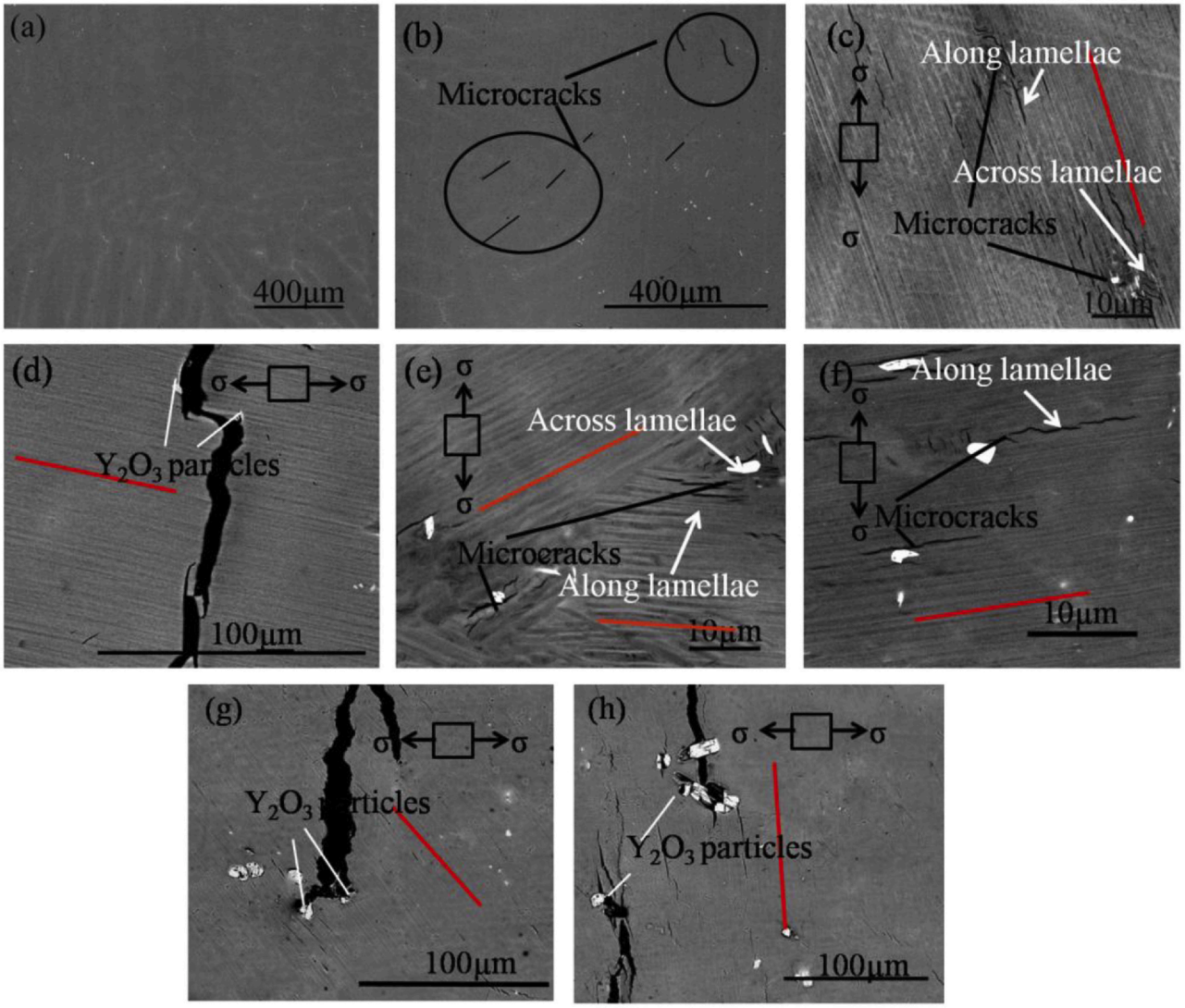

Fig. 15. Micro-cracks observed to form around yttria precipitates in a Ti-45Al-2Cr-2Nb alloy solidified in yttria molds. This interfacial mass transfer significantly impaired the tensile strength and elongation of the specimen (reprinted with permission from Ref. [108]).

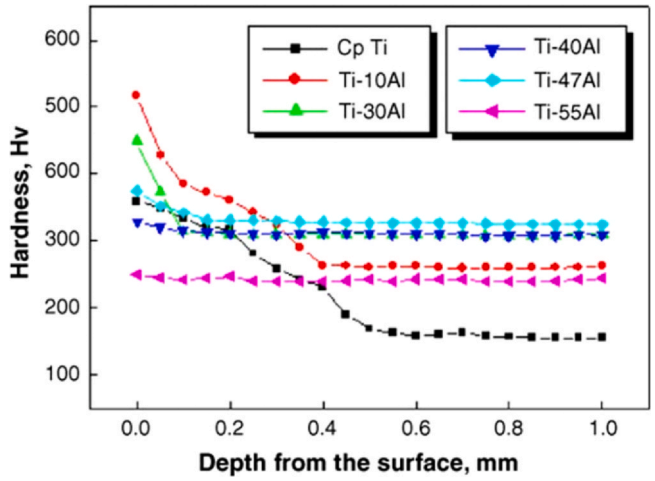

Fig. 16. Difference in surface hardness of various Ti-xAl ($0 \le x \le 55$ at%) alloys each cast in a similar alumina mold. TiAl alloys with less than 30 at% aluminum formed an α-case layer while those with more than 30 at% exhibited little to no hardness increment. This is primarily explained by the lower melting temperature of Ti-xAl alloys with a high aluminum content compared to their counterparts (reprinted with permission from Ref. [30]).

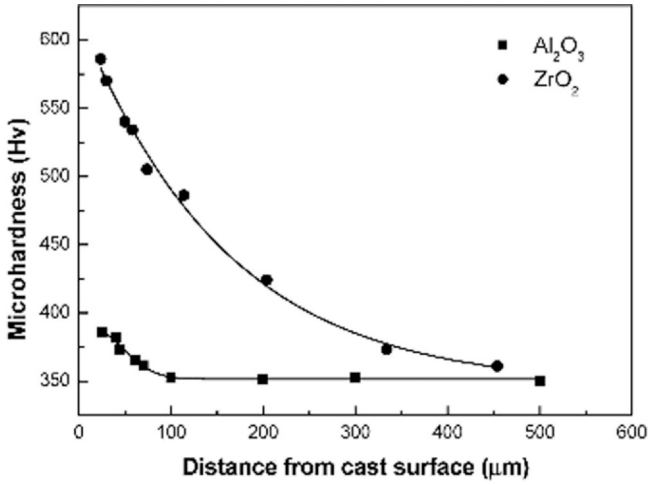

Fig. 17. Experimental results demonstrating significantly higher surface microhardness of Ti-46Al cast in a calcia-stabilized zirconia mold than in an alumina mold. This difference shows that there was less interfacial mass transfer from the alumina mold than the zirconia mold (reprinted with permission from Ref. [129]).

improving the interfacial stability of alumina molds in contact with minimally alloyed titanium melts, such as cp-Ti, by adding titanium powder or TiO_2 to the alumina mold [42,43,131]. Surprisingly, a drastic reduction in α-case thickness by a factor of seven was reported on cp-Ti cast in alumina molds with up to 50 wt% titanium powder [131]. The presence of titanium in the mold lowers the concentration gradient when in contact with a titanium alloy casting. Hence, this mitigates the interfacial mass transfer, which is in excellent agreement with the above diffusion model in Eq. (19).

Comparative studies examining thermal stability and corrosion resistance of different refractories in contact with a particular titanium alloy melt are a typical way of optimizing material selection. However, care should be taken to avoid generalizing such results to other titanium alloys. For example, in a study that compared the inertness of alumina, magnesia, calcia, and yttria refractories in contact with a γ-TiAl alloy molten at 1550 °C, the interfacial oxygen dissolution after 18 min was 9500 ppm, 9600 ppm, 2400 ppm, and 1500 ppm, respectively [106]. Even though the oxygen dissolution from alumina and magnesia were very similar, this result might be only valid for γ-TiAl. Magnesium is an alkaline earth element and has a very low solubility in pure titanium [132], but is highly soluble in aluminum [133]. Magnesia also exhibits a high magnesium vapor pressure in non-oxidizing atmospheres at high temperatures [85]. Thus, the corrosion of magnesia crucibles by the TiAl melt as reported by Kuang et al. [106] can be possibly attributed to the concurrent dissolution of magnesium and oxygen. On the other hand, the low solubility of magnesium in pure titanium in conjunction with the high vapor pressure of magnesia refractories in inert gas atmosphere make them particularly unsuitable as crucibles for titanium alloys with a low aluminum content.

4.2.2. Zirconia

As discussed in Section 2.3.3, zirconia molds are inadequately resistant to mass transfer in contact with Ti-6Al-4V or cp-Ti during investment casting [28,33]. Similar high mass transfer was also observed for Ti-46Al (at%) [129]. In this study, even though both zirconia and alumina mold elements diffused into the Ti-46Al castings, a reaction layer of at least 230 μm thickness was measured on the specimen cast in the zirconia mold, while it was less than 80 μm thick on the specimen cast in the alumina mold [129]. As a result, the degree of metal-mold reactions drastically impacted the surface microhardness as is illustrated in Fig. 17 [129]. Notably, the zirconia mold was calcia-stabilized with 0.15 mol% CaO, which could have influenced this mold's corrosion resistance. In a related study, it was found that a low calcia content of 5 mol% in ZrO_2 effectively prevented interfacial reaction with titanium at 1500 °C, while a content of 9 mol% and 17 mol% had extensive interdiffusion [134]. Furthermore, compared to a previous study [106], the binder choice of zirconia sol instead of colloidal silica greatly aided in minimizing interfacial reactions between the Ti-46Al and the alumina mold [129]. Generally, the significant reactivity between zirconia and titanium alloys would be expected because the titanium-zirconium phase diagram shows that between 600 and 1600 °C, α-Ti can dissolve up to 20 at% zirconia in solid solution [135]. In fact, the Zr-O phase diagram is very comparable to the Ti-O phase diagram as given in Fig. 6, whereas zirconium is completely soluble in titanium [136].

4.2.3. Calcia

Calcia (CaO) was one of the first materials proposed to minimize the kinetically-driven reactions between crucibles or molds in contact with titanium alloys during high temperature processing [137]. CaO has a very high melting temperature of 2899 °C and a high thermodynamic stability (exceedingly low Gibbs free energy of formation) [138]. Calcium also has a negligible dissolution in titanium, specifically, 0.006 wt% in cp-Ti at 1000 °C [101]. However, while there was exceedingly low oxygen dissolution reported in a distinct patent on CaO crucibles [139], the authors find these values to be improbable given other studies that have examined similar titanium alloys [22,87,106,140]. As displayed in Table 2, there is a contradiction of 46–65% between the results reported in the patent [139] and those obtained in earlier and later studies for cp-Ti and Ti-6Al-4V, respectively [22,87]. A literature survey summarizing oxygen contamination values from CaO when in contact with different titanium alloys is given in Table 2.

Even though calcium may hardly diffuse into titanium [134], CaO refractories react rapidly with water below 511 °C, for example from air moisture (see Eq. (23)), resulting in a substantial increase in volume and subsequent cracking of the refractory material [141]. Many ceramic oxides show excellent thermal stability and creep resistance up to 2000 °C, but they suffer from high thermal expansion making them highly susceptible to thermal shock [84,142]. A comparison among CaO, MgO, Al_2O_3 and Y_2O_3 shows that calcia has the second highest mean thermal expansion coefficient of

Table 2
Mass transfer of oxygen into titanium alloys when in contact with a CaO refractory at a temperature of 1500 °C and above (modified from Ref. [150]). [a]means dissolution values are inconceivably low.

Reference	Ti alloy	O_2 dissolution (wt%)
Li et al. [151]	TiFe	0.080–0.084
Tetsui et al. [22]	Ti-28.7Al-7Mn	0.26–0.35
Friedrich et al. [140]	Ti-50Al	0.25–0.35
	Ti-6Al-4V	Rapid dissolution/evaporation
Kuang et al. [106]	Ti-48Al-2Nb-2Mn	0.24–0.30
Degawa et al. [139][a]	cp-Ti	0.075–0.540
	Ti-6Al-4V	0.102–0.345
	Ti-20Ni	0.052–0.135
	Ti-33Al	0.036–0.062
Kroll [87]	cp-Ti	Rapid dissolution/evaporation (> 1.0)

Table 3
Mass transfer of oxygen and yttrium from yttria crucibles/molds into titanium alloys from a temperature of 1500 °C and above (modified from Ref. [150]).

Reference	Ti alloy	O_2 dissolved (wt%)	Y dissolved (wt%)
Cui et al. [159]	Ti-47Al-2Cr-2Nb	0.38	NA
Cui et al. [160]	Ti-47Al-2Cr-2Nb	0.45	0.0067
Gao et al. [161]	Ti-54Al	0.06–0.16	0.1–0.34
Gomes et al. [68]	Ti-48Al	0.16–0.23	0–0.11
Cui et al. [155]	TiAl	0.14–0.18	0.14–0.19
Tetsui et al. [162]	Ti-46Al	0.12	NA
Friedrich et al. [140]	TiAl	0.32	0.31
	Ti-6Al-4V	0.74	0.26
Saha et al. [163]	cp-Ti	0.85–1.1	0.05
Helferich and Zanis [164]	cp-Ti	0.12–0.56	0.2–1.93

15.71×10^{-6} K^{-1} from 25 to 1600 °C, only surpassed by MgO [142]. To de-oxygenate titanium alloys, it is important to know the free energy of formation for the titanium phases. The partial molar free energy of formation for oxygen dissolved in β-Ti, was determined by equilibrating Ti-O alloys with a Ca-CaO system between 1173 and 1373 K [101]. Calculations using Eq. (24) were in agreement with subsequent empirical results which showed up to 490 wt ppm O_2 dissolved in β-Ti at 1273 K.

$$CaO\,(s) + H_2O\,(g) = Ca(OH)_2\,(s) \tag{23}$$

$$\frac{1}{2}\ln\left(\frac{P_{O2}}{101325\,\mathrm{Pa}}\right) = \ln(\mathrm{wt\ \%O}) + 10.6 - \frac{70100}{T} \tag{24}$$

where P_{O_2} is the oxygen partial pressure, wt% O is the concentration of oxygen in β-Ti and T is a temperature in the range between 1173 and 1373 K [101].

A recent study remarkably lowered oxygen levels in cp-Ti and Ti-6Al-4V from 20,000 ppm to less than 1000 ppm by an enhanced use of $CaCl_2$ molten salt through a low temperature de-oxygenation process [143]. This study operated at a significantly lower temperature (as low as 600 °C), compared to previous studies which required a temperature of ≥ 900 °C to achieve optimal solid-liquid contact between calcium and titanium [144–147]. Nonetheless, there are still some major shortcomings to the industrial-scale application of calcium halide molten salts for the de-oxygenating of titanium or extracting titanium metal from TiO_2. First, laboratory-scale electro-reduction methods commonly start with commercially available TiO_2 pigment precursors [144,146], but these well-crystallized precursors are uneconomical for large-scale use. Instead, precursors like titanium-rich slag, solid metatitanic acid, and titania dust are preferred because they are cheaper [145]. Secondly, difficult-to-reduce intermediate phases such as $CaTiO_3$ and $CaTi_2O_4$, can be persistent in the kinetic pathway which significantly slows the electrochemical reduction [146,147]. Nonetheless, a similar challenge was also reported from reduction of other metal oxides such as niobium oxide and chromium oxide [148,149]. In all these studies, it was vital to understand mass transfer of the oxide ions through the solid solution towards the cathode.

4.2.4. Yttria

Yttria (Y_2O_3) is a rare earth ceramic oxide with significantly better corrosion resistance than the aforementioned refractories. For example, unlike zirconia molds which can result in a reaction layer of 200–300 μm [129,152,153], yttria molds cause only reaction layers of about 10 μm [153–155]. Furthermore, it was observed that the formation of an interfacial reaction between Y_2O_3/ZrO_2 samples in contact with a cp-Ti melt at 1700 °C was greatly hindered when at least 30 vol% Y_2O_3 was present in the samples [156]. Nonetheless, yttria is still not completely inert to titanium alloy melts as depicted by the impurity values expressed in Table 3. Not only can oxygen diffuse from the yttria lining into the titanium alloy melt, but yttrium as well [108,150,157]. Specifically, oxygen dissolution can range up to 1.6 wt% while yttrium dissolution ranges up to 1.93 wt% as summarized in Table 3.

Due to its high cost, yttria is often applied as a facecoat while the bulk material is a cheaper but less inert material like alumina or zirconia [68,106,107,158]. In such composite systems, it is important to ensure not only chemical stability between the primary facecoat and bulk materials, but also with the binders. For instance, in Y_2O_3-ZrO_2 composite investment molds, binders in the facecoat reacted with filler materials to form various oxides [158]. Such oxides included $Y_4Zr_3O_{12}$ when a zirconia sol binder was added, and $YAlO_3$, $Y_3Al_5O_{12}$ and $Y_4Al_2O_9$ when alumina sol binder was added. However, while such oxide phases could influence interfacial diffusion between the facecoats and titanium alloy castings, in this particular study, no observable reactions were seen in contact with a Ti-45Al-2Mn-2Nb-0.2B alloy at 1650 °C for 60 s under vacuum.

4.2.5. Future direction—alkaline earth ziconate materials

The current trend for advanced refractory ceramic crucibles and molds for titanium metallurgy is heading towards alkaline earth zirconates, particularly calcium zirconate ($CaZrO_3$) and barium zirconate ($BaZrO_3$) [29,55,165]. First of all, $CaZrO_3$ and $BaZrO_3$ have extremely high melting temperatures of 2368 °C and 2700 °C, respectively [85,166]. Moreover, research in recent years has demonstrated that alkaline earth materials, especially $CaZrO_3$, have remarkable corrosion resistance in contact with titanium alloys melts [21,29,55,150,167,168].

In state-of-the-art investment casting, it is vital to model and empirically analyze the impact that both crucible and shell mold materials have on the interfacial mass transfer. In a recent study that examined the coupled effect of different crucible and shell mold materials for processing Ti-6Al-4V, it was found that the alloy specimen molten in a copper crucible and cast in a $CaZrO_3$ shell mold had remarkably better surface properties than the ones using a combination of a commercially available yttria-coated crucible and silica-bonded alumina shell mold [29]. Better corrosion resistance correlated with minimal to no metal-mold reaction, which was indicated by lower surface hardness from oxygen pickup, easy demolding, and a shiny metallic appearance as demonstrated in Fig. 18. Similarly, $BaZrO_3$ also showed promising low mass transfer when used as a crucible or mold material. Fused $BaZrO_3$ crucibles were used for melting a Ti-46Al-8Nb alloy at 1550 °C and only 0.078 wt% of diffused oxygen was noted [169]. This oxygen content was favorably below the commercial threshold of 0.1 wt%. As explained earlier, a material that is successful as a crucible makes a viable mold material because of the reduced dwell time and temperature during

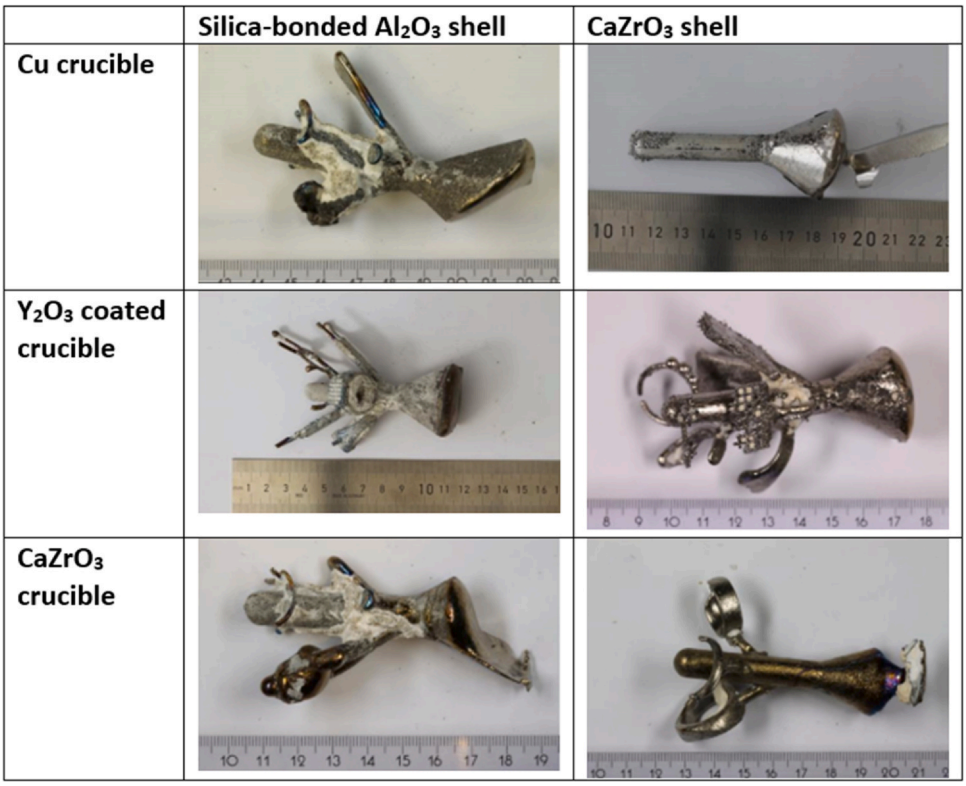

Fig. 18. A comparative analysis of different crucible and mold materials to optimize the properties of Ti-6Al-4V castings. The used crucibles were water-cooled copper, yttria and calcium zirconate respectively, while the investment molds were made of a commercial silica-bonded alumina shell and a calcium zirconate shell. The best combination was the water-cooled copper crucible and the calcium zirconate shell mold (recreated with permission from Ref. [29]).

investment casting compared to melting. Of course, other factors including ease of fabrication, cost and thermal conductivity and expansion must also be considered [74].

Alkaline earth zirconates, specifically $CaZrO_3$, also have an exceedingly low Gibbs energy of formation which is associated with a much lower alkaline earth element and vapor pressure compared to their principle oxide counterparts (CaO, SrO, BaO) [85,150,170]. This difference enables excellent thermodynamic and kinetic stability of the zirconates. Furthermore, alkaline earth zirconates have a close-packed perovskite structure. Perovskites have a general stoichiometry of ABO_3, and their AO sublattice forms a face centered cubic close-packed arrangement [171,172]. The close packed structure and thermodynamic stability of these perovskites support the low diffusion rates observed when these materials are in contact with titanium alloy melts [21,29,55,167]. On the contrary, cubic ZrO_2 has a stoichiometry of MX_2, and an open fluorite structure [171]. Additionally, cubic zirconia is noted for its large oxygen vacancy concentration [173], which could explain the high oxygen diffusion through zirconia molds [28,33,129]. Moreover, zirconia and oxygen show more than 20 at% complete solid solubility in titanium before forming an oxide [83,135], whereas $CaZrO_3$ reduces the activity of these elements [85].

4.3. Role of alloy composition on metal-mold reactions

Until now, many studies have focused on mitigating mass transfer during investment casting of titanium alloys primarily by modifying mold materials [27,29,31,43,58,160]. However, no refractory ceramic has yet been found to be completely inert. Nonetheless, few studies have thoroughly explored the effect of alloying elements on the interfacial reactivity between titanium alloy melts and ceramic oxide molds. It was particularly observed that aluminum content in TiAl alloys significantly influenced metal-mold reactions [30,105]. It was striking that Ti-xAl alloys with less than 30 at% aluminum formed pronounced α-case layers, while castings with more than 30 at% aluminum had much thinner α-case layers [30]. Consequently, this contrast led to drastic differences in surface hardness as demonstrated in Fig. 16. The aluminum content investigated in this study ranged from 0 to 55 at% aluminum, and the Ti-xAl samples were cast in Al_2O_3 molds with the same composition. This observation agreed with another study which had the turning point at 40 at% aluminum in Ti-xAl also cast in Al_2O_3 molds [105].

Presence of a high aluminum activity in the titanium alloy melt is inferred to reduce the reaction kinetics with alumina molds. Furthermore, Ti-xAl castings with $x \geq 30$ at% aluminum, are characterized with a lower melting point and a lower reactivity, thus, significantly reduced metal-mold reactions observed [30,105]. Moreover, another recent investigation reported that when melting γ-TiAl in calcium zirconate crucibles, secondary calcium aluminate phases formed on the crucible surface [174]. It can be therefore concluded that the high aluminum activity in TiAl caused the formation of calcium aluminate and dissolution of zirconium. Therefore, further studies should evaluate the effect of alloying elements on interface reactions with crucibles and molds.

4.4. Removal of alpha-case

As explained earlier, metal-mold reactions during investment casting of titanium alloys leave a hard and brittle α-case layer beneath the oxide [27,29,31–33,93]. The thickness of the α-case is a function of time, temperature and availability of oxygen [28,175]. Current methods to remove this reaction layer include mechanical grinding, laser irradiation, water jetting, cathodic de-oxygenation and chemical milling [46–50]. However, α-case removal processes

increase manufacturing time and cost, and some may impair surface properties of cast titanium alloys. For example, chemical milling caused pitting and grain boundary corrosion on the surface of cast Ti-6242 alloy specimens, which significantly decreased their low cycle fatigue life [176]. Therefore, it is important to investigate mass transfer involved in investment casting of titanium alloys in order to minimize the cost-intensive post-casting processes and to achieve titanium alloy castings with excellent surface properties and near-net shape.

Cost-efficiency improvements from minimizing the necessity of removing unwanted α-case layers, could expedite adoption of titanium alloys not only for high-end uses (aerospace, biomedical), but also for automotive applications and hydrogen storage. Laboratory-scale studies already showed that TiAl alloys are great substitute materials for exhaust car valves [82,109]. A change from steel to titanium vehicle parts would significantly reduce weight, lower fuel consumption and reduce gas emissions. Secondly, TiFe is a studied and promising alloy for hydrogen storage [151]. Hydrogen storage materials are attractive for state-of-the-art fuel cell-powered vehicles, as well as portable and stationary power industries. Nonetheless, mass transfer of contaminants during the melting of TiFe alloys is still a challenge, generating reaction layers of up to 200 μm when melted in a graphite crucible. However, it was observed that calcium oxide could be a promising alternative refractory for processing TiFe alloys [151].

5. Conclusions and future prospects

Titanium alloys have highly desirable properties like exceptional corrosion resistance, low density, and high specific strength. therefore, they are increasingly applied in aerospace, chemical, and biomedical applications. Novel research is also diversifying the use of TiAl and TiFe alloys for automotive applications to lower emissions. Nonetheless, processing of titanium alloys still suffers from mass transfer challenges, which affect the structure and properties of the alloy parts. Future research in investment casting should optimize the mold and alloy composition design to decrease manufacturing costs and foster wider application of titanium alloys. After investigating how these challenges can be addressed, the following conclusions were drawn.

- Analysis of transport phenomena involved in processing by using models and simulations has been beneficial for improved products and cost efficiency. Mass transfer is particularly problematic in investment casting of titanium alloys because these alloys are highly reactive in molten state. Oxygen diffusion during processing significantly affects the microstructure and mechanical properties of the casting—the surface hardness drastically increases, and fracture toughness decreases. Moreover, internal inclusions act as stress concentrators which facilitate crack propagation in the cast part, thus, lowering its fatigue resistance.
- State-of-the-art investment casting often utilizes centrifugal mold filling instead of gravity mold filling especially for manufacturing of thin castings with complex shapes. In this review, models and experimental studies of both types of investment casting were examined, and it was seen that centrifugal investment casting yields less shrinkage porosity and stress cracks.
- Properties of successful crucible and mold materials include a high melting temperature, low vapor pressure, chemical stability, creep resistance, and thermal shock resistance. Oxide refractories have shown higher corrosion resistance in contact with titanium alloys than carbide, nitride, and boride ceramics, therefore, they are preferred for investment casting. Nonetheless, even ceramic oxides are not completely inert to titanium alloy melts. Composite molds have been suggested, but further research is needed to limit bulk material diffusion into the castings.
- Promising refractories for optimizing resistance to interfacial oxide diffusion during casting, are characterized by very low Gibbs free energy and a perovskite structure. These include alkaline earth zirconates namely, $CaZrO_3$ or $BaZrO_3$, and they have shown significantly better corrosion resistance than many commercially available molds. Nevertheless, these materials are still in the developmental stage, and more work is needed to fully characterize their creep and thermal shock resistance.

Declaration of Competing Interest

The authors declare that they have no known competing financial interests or personal relationships that could have appeared to influence the work reported in this paper.

Acknowledgment

The authors would like to thank the Institute of Material Science (IMS) and the School of Engineering of the University of Connecticut for faculty startup funds.

References

[1] A. Mahashabde, P. Wolfe, A. Ashok, C. Dorbian, Q. He, A. Fan, S. Lukachko, A. Mozdzanowska, C. Wollersheim, S.R. Barrett, M. Locke, I. Waitz, Assessing the environmental impacts of aircraft noise and emissions, Prog. Aerosp. Sci. 47 (2011) 15–52, https://doi.org/10.1016/j.paerosci.2010.04.003
[2] M. Marino, R. Sabatini, Advanced lightweight aircraft design configurations for green operations, in: Practical Responses to Climate Change Conference 2014, Engineers Australia, 2014, pp. 207–215.
[3] H. Clemens, S. Mayer, Design, processing, microstructure, properties, and applications of advanced intermetallic TiAl alloys, Adv. Eng. Mater. 15 (2013) 191–215, https://doi.org/10.1002/adem.201200231
[4] M.F. Ashby, D.R.H. Jones, Engineering Materials 1: An Introduction to Properties, Applications and Design, first ed, Elsevier, 2012.
[5] H. Clemens, W. Wallgram, S. Kremmer, V. Güther, A. Otto, A. Bartels, Design of novel β -solidifying TiAl alloys with adjustable β/B2 -phase fraction and excellent hot-workability, Adv. Eng. Mater. 10 (2008) 707–713, https://doi.org/10.1002/adem.200800164
[6] M. Reytier, F. Kircher, B. Levesy, Characterization of titanium alloys for cryogenic applications, AIP Conf. Proc. 614 (2002) 76–83. doi:10.1063/1.1472528.
[7] M. Niinomi, M. Nakai, J. Hieda, Development of new metallic alloys for biomedical applications, Acta Biomater. 8 (2012) 3888–3903, https://doi.org/10.1016/j.actbio.2012.06.037
[8] M. Geetha, A.K. Singh, R. Asokamani, A.K. Gogia, Ti based biomaterials, the ultimate choice for orthopaedic implants-a review, Prog. Mater. Sci. 54 (2009) 397–425, https://doi.org/10.1016/j.pmatsci.2008.06.004
[9] N. Manam, W. Harun, D. Shri, S. Ghani, T. Kurniawan, M.H. Ismail, M. Ibrahim, Study of corrosion in biocompatible metals for implants: a review, J. Alloy. Compd. 701 (2017) 698–715, https://doi.org/10.1016/j.jallcom.2017.01.196
[10] H. Liu, M. Niinomi, M. Nakai, S. Obara, H. Fujii, Improved fatigue properties with maintaining low Young's modulus achieved in biomedical beta-type titanium alloy by oxygen addition, Mater. Sci. Eng. A 704 (2017) 10–17, https://doi.org/10.1016/j.msea.2017.07.078
[11] D. Banerjee, J. Williams, Perspectives on titanium science and technology, Acta Mater. 61 (2013) 844–879, https://doi.org/10.1016/j.actamat.2012.10.043
[12] B. Daley, A. Doherty, B. Fairman, C. Case, Wear debris from hip or knee replacements causes chromosomal damage in human cells in tissue culture, J. Bone Jt. Surg. 86 (2004) 598–606, https://doi.org/10.1302/0301-620X.86B4.14368
[13] P.R. Walker, J. LeBlanc, M. Sikorska, Effects of aluminum and other cations on the structure of brain and liver chromatin, Biochemistry 28 (1989) 3911–3915, https://doi.org/10.1021/bi00435a043
[14] C.A.R. Maestro, A.H.S. Bueno, A.M. de Sousa Malafaia, Cyclic thermal oxidation evaluation to improve Ti-6Al-4V surface in applications as biomaterial, J. Mater. Eng. Perform. 28 (2019) 4991–4997, https://doi.org/10.1007/s11665-019-04220-x
[15] S.J. Sullivan, L.T. Topoleski, Surface modifications for improved wear performance in artificial joints: a review, JOM 67 (2015) 2502–2517, https://doi.org/10.1007/s11837-015-1543-0
[16] K. Aniołek, Structure and properties of titanium and the Ti-6Al-7Nb alloy after isothermal oxidation, Surf. Eng. (2020) 1–12, https://doi.org/10.1080/02670844.2020.1711631
[17] S. Pattnaik, D.B. Karunakar, P. Jha, Developments in investment casting process: a review, J. Mater. Process. Technol. 212 (2012) 2332–2348, https://doi.org/10.1016/j.jmatprotec.2012.06.003
[18] L. Nastac, M. Gungor, I. Ucok, K. Klug, W.T. Tack, Advances in investment casting of Ti-6Al-4V: a review, Int. J. Cast Met. Res. 19 (2006) 73–93, https://doi.org/10.1179/136404605225023225

[19] R. Harding, M. Wickins, H. Wang, G. Djambazov, K. Pericleous, Development of a turbulence-free casting technique for titanium aluminides, Intermetallics 19 (2011) 805–813, https://doi.org/10.1016/j.intermet.2010.11.022

[20] J. Ou, S.L. Cockcroft, D.M. Maijer, L. Yao, C. Reilly, A. Akhtar, An examination of the factors influencing the melting of solid titanium in liquid titanium, Int. J. Heat Mass Transf. 86 (2015) 221–233, https://doi.org/10.1016/j.ijheatmasstransfer.2015.02.054

[21] S. Schafföner, M. Bach, C. Jahn, L. Freitag, C.G. Aneziris, Advanced refractories for titanium metallurgy based on calcium zirconate with improved thermomechanical properties, J. Eur. Ceram. Soc. 39 (2019) 4394–4403, https://doi.org/10.1016/j.jeurceramsoc.2019.06.007

[22] T. Tetsui, T. Kobayashi, T. Ueno, H. Harada, Consideration of the influence of contamination from oxide crucibles on TiAl cast material, and the possibility of achieving low-purity TiAl precision cast turbine wheels, Intermetallics 31 (2012) 274–281, https://doi.org/10.1016/j.intermet.2012.07.019

[23] A. Fadeev, V. Bazhenov, A. Koltygin, Improvement in the casting technology of blades for aviation gas-turbine engines made of TNM-B1 titanium aluminide alloy produced by induction crucible melting, Russ. J. Non-ferr. Met. 56 (2015) 26–32, https://doi.org/10.3103/S1067821215010071

[24] K. Kamyshnykova, J. Lapin, Vacuum induction melting and solidification of TiAl-based alloy in graphite crucibles, Vacuum 154 (2018) 218–226, https://doi.org/10.1016/j.vacuum.2018.05.017

[25] C. Frueh, D.R. Poirier, M. Maguire, R. Harding, Attempts to develop a ceramic mould for titanium casting-a review, Int. J. Cast Met. Res. 9 (1996) 233–239, https://doi.org/10.1080/13640461.1996.11819664

[26] X. Cheng, C. Yuan, D. Shevchenko, P. Withey, The influence of mould pre-heat temperature and casting size on the interaction between a Ti-46Al-8Nb-1B alloy and the mould comprising an Al_2O_3 face coat, Mater. Chem. Phys. 146 (2014) 295–302, https://doi.org/10.1016/j.matchemphys.2014.03.026

[27] X. Chamorro, N. Herrero-Dorca, P. Rodríguez, U. Andrés, Z. Azpilgain, α-case formation in Ti-6Al-4V investment casting using $ZrSiO_4$ and Al_2O_3 moulds, J. Mater. Process. Technol. 243 (2017) 75–81, https://doi.org/10.1016/j.jmatprotec.2016.12.007

[28] A.H. Liu, B.S. Li, Y.W. Sui, J.J. Guo, Numerical simulation of interfacial reaction between titanium and zirconia, China Foundry 7 (2010) 373–376.

[29] U.E. Klotz, C. Legner, F. Bulling, L. Freitag, C. Faßauer, S. Schafföner, C. Aneziris, Investment casting of titanium alloys with calcium zirconate moulds and crucibles, Int. J. Adv. Manuf. Technol. (2019) 1–11, https://doi.org/10.1007/s00170-019-03538-z

[30] S.-Y. Sung, Y.-J. Kim, Influence of Al contents on alpha-case formation of Ti-xAl alloys, J. Alloy. Compd. 415 (2006) 93–98, https://doi.org/10.1016/j.jallcom.2005.07.051

[31] G. Yu, N. Li, Y. Li, Y. Wang, The effects of different types of investments on the alpha-case layer of titanium castings, J. Prosthet. Dent. 97 (2007) 157–164, https://doi.org/10.1016/j.prosdent.2007.01.005

[32] S.-Y. Sung, Y.-J. Kim, Alpha-case formation mechanism on titanium investment castings, Mater. Sci. Eng. A 405 (2005) 173–177, https://doi.org/10.1016/j.msea.2005.05.092

[33] W.J. Boettinger, M.E. Williams, S.R. Coriell, U.R. Kattner, B. Mueller, Alpha case thickness modeling in investment castings, Met. Mater. Trans. B 31 (2000) 1419–1427, https://doi.org/10.1007/s11663-000-0026-y

[34] D.P. Satko, J.B. Shaffer, J.S. Tiley, S.L. Semiatin, A.L. Pilchak, S.R. Kalidindi, Y. Kosaka, M.G. Glavicic, A.A. Salem, Effect of microstructure on oxygen rich layer evolution and its impact on fatigue life during high-temperature application of α/β titanium, Acta Mater. 107 (2016) 377–389, https://doi.org/10.1016/j.actamat.2016.01.058

[35] S. Semiatin, T. Lehner, J. Miller, R. Doherty, D. Furrer, Alpha/beta heat treatment of a titanium alloy with a nonuniform microstructure, Met. Mater. Trans. A 38 (2007) 910–921, https://doi.org/10.1007/s11661-007-9088-7

[36] S. Semiatin, S. Knisley, P. Fagin, D. Barker, F. Zhang, Microstructure evolution during alpha-beta heat treatment of Ti-6Al-4V, Met. Mater. Trans. A 34 (2003) 2377–2386, https://doi.org/10.1007/s11661-003-0300-0

[37] R. Gaddam, B. Sefer, R. Pederson, M.-L. Antti, Oxidation and alpha-case formation in Ti-6Al-2Sn-4Zr-2Mo alloy, Mater. Charact. 99 (2015) 166–174, https://doi.org/10.1016/j.matchar.2014.11.023

[38] T. Parthasarathy, W. Porter, S. Boone, R. John, P. Martin, Life prediction under tension of titanium alloys that develop an oxygenated brittle case during use, Scr. Mater. 65 (2011) 420–423, https://doi.org/10.1016/j.scriptamat.2011.05.025

[39] S. Zabler, Interstitial oxygen diffusion hardening-a practical route for the surface protection of titanium, Mater. Charact. 62 (2011) 1205–1213, https://doi.org/10.1016/j.matchar.2011.10.012

[40] J. Qu, P.J. Blau, J.Y. Howe, H.M. Meyer III, Oxygen diffusion enables anti-wear boundary film formation on titanium surfaces in zinc-dialkyl-dithiophosphate (ZDDP)-containing lubricants, Scr. Mater. 60 (2009) 886–889, https://doi.org/10.1016/j.scriptamat.2009.02.009

[41] R. Yazdi, H. Ghasemi, C. Wang, A. Neville, Bio-corrosion behaviour of oxygen diffusion layer on Ti-6Al-4V during tribocorrosion, Corros. Sci. 128 (2017) 23–32, https://doi.org/10.1016/j.corsci.2017.08.031

[42] S. Lee, Y.-J. Kim, Evaluation of the α-case with TiO_2 in mold for titanium investment casting, Int. J. Metalcast. 11 (2017) 71–76, https://doi.org/10.1007/s40962-016-0093-8

[43] B.-J. Choi, S. Lee, Y.-J. Kim, Alpha-case reduction mechanism of titanium powder-added investment molds for titanium casting, J. Mater. Eng. Perform. 23 (2014) 1415–1423, https://doi.org/10.1007/s11665-013-0859-6

[44] R. Gaddam, M.-L. Antti, R. Pederson, Influence of alpha-case layer on the low cycle fatigue properties of Ti-6Al-2Sn-4Zr-2Mo alloy, Mater. Sci. Eng. A 599 (2014) 51–56, https://doi.org/10.1016/j.msea.2014.01.059

[45] Z. Abdallah, K. Perkins, S. Williams, Alpha-case kinetics and surface crack growth in the high-temperature alloy TIMETAL 834 under creep conditions, Met. Mater. Trans. A 43 (2012) 4647–4654, https://doi.org/10.1007/s11661-012-1285-3

[46] M. Koike, D. Jacobson, K.S. Chan, T. Okabe, Grindability of alpha-case formed on cast titanium, Dent. Mater. J. 28 (2009) 587–594, https://doi.org/10.4012/dmj.28.587

[47] L. Yue, Z. Wang, L. Li, Material morphological characteristics in laser ablation of alpha case from titanium alloy, Appl. Surf. Sci. 258 (2012) 8065–8071, https://doi.org/10.1016/j.apsusc.2012.04.173

[48] L. Huang, P. Kinnell, P. Shipway, Parametric effects on grit embedment and surface morphology in an innovative hybrid waterjet cleaning process for alpha case removal from titanium alloys, Procedia CIRP 6 (2013) 594–599, https://doi.org/10.1016/j.procir.2013.03.077

[49] G.Z. Chen, D.J. Fray, T.W. Farthing, Cathodic deoxygenation of the alpha case on titanium and alloys in molten calcium chloride, Met. Mater. Trans. B 32 (2001) 1041–1052, https://doi.org/10.1007/s11663-001-0093-8

[50] V. Deshmukh, R. Kadam, S.S. Joshi, Removal of alpha case on titanium alloy surfaces using chemical milling, Mach. Sci. Technol. 21 (2017) 257–278, https://doi.org/10.1080/10910344.2017.1284558

[51] S. Wang, A. Miranda, C. Shih, A study of investment casting with plastic patterns, Mater. Manuf. Process. 25 (2010) 1482–1488, https://doi.org/10.1080/10426914.2010.529585

[52] W. Yao, M.C. Leu, Analysis of shell cracking in investment casting with laser stereolithography patterns, Rapid Prototyp. J. (1999).

[53] W. Everhart, S. Lekakh, V. Richards, J. Chen, K. Chandrashekhara, Crack formation during foam pattern firing in the investment casting process, Int. J. Metalcast. 7 (2013) 7–14, https://doi.org/10.1007/BF03355549

[54] A. Kostov, B. Friedrich, Predicting thermodynamic stability of crucible oxides in molten titanium and titanium alloys, Comput. Mater. Sci. 38 (2006) 374–385, https://doi.org/10.1016/j.commatsci.2006.03.006

[55] S. Schafföner, C.G. Aneziris, H. Berek, B. Rotmann, B. Friedrich, Investigating the corrosion resistance of calcium zirconate in contact with titanium alloy melts, J. Eur. Ceram. Soc. 35 (2015) 259–266, https://doi.org/10.1016/j.jeurceramsoc.2014.08.031

[56] I.P. Nanda, Z. Ali, M.H. Idris, A. Arafat, A. Pratoto, Shell mould strength of rice husk ash (RHA) and bentonite clays in investment casting, Int. J. Adv. Sci. Eng. Inf. Technol. 8 (2018) 291–297, https://doi.org/10.18517/ijaseit.8.1.4209

[57] R. Prasad, Progress in investment castings, Science and Technology of Casting Processes, IntechOpen, 2012, pp. 25–72.

[58] M.-G. Kim, S.K. Kim, Y.-J. Kim, Effect of mold material and binder on metal-mold interfacial reaction for investment castings of titanium alloys, Mater. Trans. 43 (2002) 745–750, https://doi.org/10.15623/ijret.2014.0310005

[59] C. Frueh, D.R. Poirier, M. Maguire, The effect of silica-containing binders on the titanium/face coat reaction, Met. Mater. Trans. B 28 (1997) 919–926, https://doi.org/10.1007/s11663-997-0019-1

[60] L. Freitag, S. Schafföner, N. Lippert, C. Fassauer, C.G. Aneziris, C. Legner, U.E. Klotz, Silica-free investment casting molds based on calcium zirconate, Ceram. Int. 43 (2017) 6807–6814, https://doi.org/10.1016/j.ceramint.2017.02.098

[61] S. Schafföner, L. Freitag, J. Hubálková, C.G. Aneziris, Functional composites based on refractories produced by pressure slip casting, J. Eur. Ceram. Soc. 36 (2016) 2109–2117, https://doi.org/10.1016/j.jeurceramsoc.2016.02.008

[62] L. Freitag, S. Schafföner, C. Faßauer, C.G. Aneziris, Functional coatings for titanium casting molds using the replica technique, J. Eur. Ceram. Soc. 38 (2018) 4560–4567, https://doi.org/10.1016/j.jeurceramsoc.2018.05.020

[63] L. Ponsonnet, K. Reybier, N. Jaffrezic, V. Comte, C. Lagneau, M. Lissac, C. Martelet, Relationship between surface properties (roughness, wettability) of titanium and titanium alloys and cell behaviour, Mater. Sci. Eng. C 23 (2003) 551–560, https://doi.org/10.1016/S0928-4931(03)00033-X

[64] M. Lai, Y. Gao, B. Yuan, M. Zhu, Remarkable superelasticity of sintered Ti-Nb alloys by Ms adjustment via oxygen regulation, Mater. Des. 87 (2015) 466–472, https://doi.org/10.1016/j.matdes.2015.07.180

[65] R. Harding, M. Wickins, Temperature measurements during induction skull melting of titanium aluminide, Mater. Sci. Technol. 19 (2003) 1235–1246, https://doi.org/10.1179/026708303225005944

[66] T. Rosenqvist, Principles of Extractive Metallurgy, Tapir Academic Press, 2004.

[67] K. Sakamoto, K. Yoshikawa, T. Kusamichi, T. Onoye, Changes in oxygen contents of titanium aluminides by vacuum induction, cold crucible induction and electron beam melting, ISIJ Int. 32 (1992) 616–624, https://doi.org/10.2355/isijinternational.32.616

[68] F. Gomes, H. Puga, J. Barbosa, C.S. Ribeiro, Effect of melting pressure and superheating on chemical composition and contamination of yttria-coated ceramic crucible induction melted titanium alloys, J. Mater. Sci. 46 (2011) 4922–4936, https://doi.org/10.1007/s10853-011-5405-z

[69] L. Yang, L. Chai, Y. Liang, Y. Zhang, C. Bao, S. Liu, J. Lin, Numerical simulation and experimental verification of gravity and centrifugal investment casting low pressure turbine blades for high Nb-TiAl alloy, Intermetallics 66 (2015) 149–155, https://doi.org/10.1016/j.intermet.2015.07.006

[70] J. Bundy, S. Viswanathan, Characterization of zircon-based slurries for investment casting, Int. J. Metalcast. 3 (2009) 27–37, https://doi.org/10.1007/BF03355439

[71] S. Jones, C. Yuan, Advances in shell moulding for investment casting, J. Mater. Process. Technol. 135 (2003) 258–265, https://doi.org/10.1016/S0924-0136(02)00907-X

[72] W. Everhart, S. Lekakh, V. Richards, J. Chen, H. Li, K. Chandrashekhara, Corner strength of investment casting shells, Int. J. Metalcast. 7 (2013) 21–27, https://doi.org/10.1007/BF03355541

[73] D.M. Kline, Controlling Strength and Permeability of Silica Investment Casting Molds (Master's thesis), Missouri University of Science and Technology, 2010. ⟨https://scholarsmine.mst.edu/masters_theses/4866/⟩.

[74] J.E. Kanyo, S. Schafföner, R.S. Uwanyuze, K.S. Leary, An overview of ceramic molds for investment casting of nickel superalloys, J. Eur. Ceram. Soc. 40 (2020) 4955–4973, https://doi.org/10.1016/j.jeurceramsoc.2020.07.013

[75] S. Jones, M. Jolly, K. Lewis, Development of techniques for predicting ceramic shell properties for investment casting, Br. Ceram. Trans. 101 (2002) 106–113, https://doi.org/10.1179/096797802225003316

[76] H. Rønold, S. Lyngstadaas, J. Ellingsen, Analysing the optimal value for titanium implant roughness in bone attachment using a tensile test, Biomaterials 24 (2003) 4559–4564, https://doi.org/10.1016/S0142-9612(03)00256-4

[77] D.A. Armitage, D.M. Grant, Characterisation of surface-modified nickel titanium alloys, Mater. Sci. Eng. A 349 (2003) 89–97, https://doi.org/10.1016/S0921-5093(02)00818-3

[78] D. MacDonald, B. Rapuano, N. Deo, M. Stranick, P. Somasundaran, A. Boskey, Thermal and chemical modification of titanium-aluminum-vanadium implant materials: effects on surface properties, glycoprotein adsorption, and MG63 cell attachment, Biomaterials 25 (2004) 3135–3146, https://doi.org/10.1016/j.biomaterials.2003.10.029

[79] L. Ponsonnet, V. Comte, A. Othmane, C. Lagneau, M. Charbonnier, M. Lissac, N. Jaffrezic, Effect of surface topography and chemistry on adhesion, orientation and growth of fibroblasts on nickel-titanium substrates, Mater. Sci. Eng. C 21 (2002) 157–165, https://doi.org/10.1016/S0928-4931(02)00097-8

[80] N. Humphreys, D. McBride, D. Shevchenko, T. Croft, P. Withey, N. Green, M. Cross, Modelling and validation: casting of Al and TiAl alloys in gravity and centrifugal casting processes, Appl. Math. Model. 37 (2013) 7633–7643, https://doi.org/10.1016/j.apm.2013.03.030

[81] C. Li, S. Wu, J. Guo, Y. Su, H. Fu, Castability of thin walled titanium alloy castings in vertical centrifugal field, Mater. Sci. Technol. 24 (2008) 1209–1213, https://doi.org/10.1179/174328407×161349

[82] P. Fu, X. Kang, Y. Ma, K. Liu, D. Li, Y. Li, Centrifugal casting of TiAl exhaust valves, Intermetallics 16 (2008) 130–138, https://doi.org/10.1016/j.intermet.2007.08.007

[83] M. Cancarevic, M. Zinkevich, F. Aldinger, Thermodynamic description of the Ti-O system using the associate model for the liquid phase, Calphad 31 (2007) 330–342, https://doi.org/10.1016/j.calphad.2007.01.009

[84] R. Raj, Fundamental research in structural ceramics for service near 2000 °C, J. Am. Ceram. Soc. 76 (1993) 2147–2174. doi:10.1111/j.1151–2916.1993.tb07750.x.

[85] N.S. Jacobson, Thermodynamic properties of some metal oxide-zirconia systems, Technical Report, NASA, 1989. ⟨https://ntrs.nasa.gov/archive/nasa/casi.ntrs.nasa.gov/19900004350.pdf⟩.

[86] W. Kroll, Method for manufacturing titanium and alloys thereof, 1940. USA Patent 2,205,854.

[87] W. Kroll, The production of ductile titanium, J. Electrochem. Soc. 78 (1940) 35–47, https://doi.org/10.1149/1.3071290

[88] C. Ouchi, H. Iizumi, S. Mitao, Effects of ultra-high purification and addition of interstitial elements on properties of pure titanium and titanium alloy, Mater. Sci. Eng. A 243 (1998) 186–195, https://doi.org/10.1016/S0921-5093(97)00799-5

[89] Z. Liu, G. Welsch, Literature survey on diffusivities of oxygen, aluminum, and vanadium in alpha titanium, beta titanium, and in rutile, Metall. Trans. A 19 (1988) 1121–1125, https://doi.org/10.1007/BF02628396

[90] A.I. Kahveci, G.E. Welsch, Effect of oxygen on the hardness and alpha/beta phase ratio of Ti-6Al-4V alloy, Scr. Metall. 20 (1986) 1287–1290, https://doi.org/10.1016/0036-9748(86)90050-5

[91] C. Oskay, M. Haney, Computational modeling of titanium structures subjected to thermo-chemo-mechanical environment, Int. J. Solids Struct. 47 (2010) 3341–3351, https://doi.org/10.1016/j.ijsolstr.2010.08.014

[92] K.S. Chan, M. Koike, B.W. Johnson, T. Okabe, Modeling of alpha-case formation and its effects on the mechanical properties of titanium alloy castings, Met. Mater. Trans. A 39 (2008) 171–180, https://doi.org/10.1007/s11661-007-9406-0

[93] R.C. Atwood, P.D. Lee, R. Curtis, Modeling the surface contamination of dental titanium investment castings, Dent. Mater. 21 (2005) 178–186, https://doi.org/10.1016/j.dental.2004.02.010

[94] R.C. Atwood, P.D. Lee, R. Curtis, D.M. Maijer, Modeling the investment casting of a titanium crown, Dent. Mater. 23 (2007) 60–70, https://doi.org/10.1016/j.dental.2005.12.001

[95] S. Teoh, Fatigue of biomaterials: a review, Int. J. Fatigue 22 (2000) 825–837, https://doi.org/10.1016/S0142-1123(00)00052-9

[96] D. Correa, P. Kuroda, M. Lourenço, M.A.R. Buzalaf, C. Grandini, Adjustment of the microstructure and selected mechanical properties of biomedical Ti-15Zr-Mo alloys through oxygen doping, J. Alloy. Compd. 775 (2019) 158–167, https://doi.org/10.1016/j.jallcom.2018.10.105

[97] R.G. Hennig, D.R. Trinkle, J. Bouchet, S.G. Srinivasan, R.C. Albers, J.W. Wilkins, Impurities block the α to ω martensitic transformation in titanium, Nat. Mater. 4 (2005) 129–133, https://doi.org/10.1038/nmat1292

[98] D. Li, W. Wan, L. Zhu, Y. Jiang, S. Shao, G. Yang, H. Liu, D. Yi, S. Cao, Q. Hu, Experimental and DFT characterization of interphase boundaries in titanium and the implications for ω-assisted α phase precipitation, Acta Mater. 151 (2018) 406–415, https://doi.org/10.1016/j.actamat.2018.03.056

[99] G. Lütjering, J.C. Williams, Titanium, Springer Science & Business Media, 2007.

[100] K. Chou, E.A. Marquis, Oxygen effects on ω and α phase transformations in a metastable β Ti-Nb alloy, Acta Mater. 181 (2019) 367–376, https://doi.org/10.1016/j.actamat.2019.09.049

[101] T.H. Okabe, R.O. Suzuki, T. Oishi, K. Ono, Thermodynamic properties of dilute titanium-oxygen solid solution in beta phase, Mater. Trans. JIM 32 (1991) 485–488, https://doi.org/10.2320/matertrans1989.32.485

[102] J. Zollinger, J. Lapin, D. Daloz, H. Combeau, Influence of oxygen on solidification behaviour of cast TiAl-based alloys, Intermetallics 15 (2007) 1343–1350, https://doi.org/10.1016/j.intermet.2007.04.002

[103] S.-Y. Sung, B.-S. Han, Y.-J. Kim, Formation of alpha case mechanism on titanium investment cast parts, Titanium Alloys-Towards Achieving Enhanced Properties for Diversified Applications, (2012), https://doi.org/10.5772/35496

[104] I. Cvijović-Alagić, Z. Cvijovi, S. Mitrović, M. Rakin, D. Veljović, M. Babić, Tribological behaviour of orthopaedic Ti-13Nb-13Zr and Ti-6Al-4V alloys, Tribol. Lett. 40 (2010) 59–70, https://doi.org/10.1007/s11249-010-9639-8

[105] M.-G. Kim, Y.-J. Kim, Investigation of interface reaction between TiAl alloys and mold materials, Met. Mater. Int. 8 (2002) 289–293, https://doi.org/10.1007/BF03186098

[106] J. Kuang, R. Harding, J. Campbell, Investigation into refractories as crucible and mould materials for melting and casting γ-TiAl alloys, J. Mater. Sci. Technol. 16 (2000) 1007–1016, https://doi.org/10.1179/026708300101508964

[107] E. Zhao, F. Kong, Y. Chen, B. Li, Interfacial reactions between Ti-1100 alloy and ceramic mould during investment casting, Trans. Nonferr. Met. Soc. China 21 (2011) 348–352, https://doi.org/10.1016/S1003-6326(11)61604-X

[108] H. Zhang, H. Ding, Q. Wang, R. Chen, J. Guo, Microstructures and tensile properties of directionally solidified Ti-45Al-2Cr-2Nb alloy by electromagnetic cold crucible zone melting technology with Y_2O_3 moulds, Vacuum 148 (2018) 206–213, https://doi.org/10.1016/j.vacuum.2017.11.032

[109] K. Gebauer, Performance, tolerance and cost of TiAl passenger car valves, Intermetallics 14 (2006) 355–360, https://doi.org/10.1016/j.intermet.2005.08.009

[110] V. Sheremetyev, V. Brailovski, S. Prokoshkin, K. Inaekyan, S. Dubinskiy, Functional fatigue behavior of superelastic beta Ti-22Nb-6Zr (at%) alloy for load-bearing biomedical applications, Mater. Sci. Eng. C 58 (2016) 935–944, https://doi.org/10.1016/j.msec.2015.09.060

[111] R.M. Pilliar, Modern metal processing for improved load-bearing surgical implants, Biomaterials 12 (1991) 95–100, https://doi.org/10.1016/0142-9612(91)90185-D

[112] T. Akahori, M. Niinomi, H. Fukui, M. Ogawa, H. Toda, Improvement in fatigue characteristics of newly developed beta type titanium alloy for biomedical applications by thermo-mechanical treatments, Mater. Sci. Eng. C 25 (2005) 248–254, https://doi.org/10.1016/j.msec.2004.12.007

[113] M. Niinomi, Recent research and development in titanium alloys for biomedical applications and healthcare goods, Sci. Technol. Adv. Mater. 4 (2003) 445, https://doi.org/10.1016/j.stam.2003.09.002

[114] J.-Y. Rho, T.Y. Tsui, G.M. Pharr, Elastic properties of human cortical and trabecular lamellar bone measured by nanoindentation, Biomaterials 18 (1997) 1325–1330, https://doi.org/10.1016/S0142-9612(97)00073-2

[115] M. Niinomi, Fatigue performance and cyto-toxicity of low rigidity titanium alloy, Ti-29Nb-13Ta-4.6Zr, Biomaterials 24 (2003) 2673–2683, https://doi.org/10.1016/S0142-9612(03)00069-3

[116] M. Niinomi, T. Hattori, K. Morikawa, T. Kasuga, A. Suzuki, H. Fukui, S. Niwa, Development of low rigidity β-type titanium alloy for biomedical applications, Mater. Trans. 43 (2002) 2970–2977, https://doi.org/10.2320/matertrans.43.2970

[117] M. Nakai, M. Niinomi, T. Oneda, Improvement in fatigue strength of biomedical β-type Ti-Nb-Ta-Zr alloy while maintaining low Young's modulus through optimizing ω-phase precipitation, Met. Mater. Trans. A 43 (2012) 294–302, https://doi.org/10.1007/s11661-011-0860-3

[118] F.B. Vicente, D. Correa, T.A. Donato, V.E. Arana-Chavez, M.A. Buzalaf, C.R. Grandini, The influence of small quantities of oxygen in the structure, microstructure, hardness, elasticity modulus and cytocompatibility of Ti-Zr alloys for dental applications, Materials 7 (2014) 542–553, https://doi.org/10.3390/ma7010542

[119] D. Velten, V. Biehl, F. Aubertin, B. Valeske, W. Possart, J. Breme, Preparation of TiO_2 layers on cp-Ti and Ti-6Al-4V by thermal and anodic oxidation and by sol-gel coating techniques and their characterization, J. Biomed. Mater. Res. 59 (2002) 18–28, https://doi.org/10.1002/jbm.1212

[120] M. Niinomi, Mechanical properties of biomedical titanium alloys, Mater. Sci. Eng. A 243 (1998) 231–236, https://doi.org/10.1016/S0921-5093(97)00806-X

[121] V. Goriainov, R. Cook, J.M. Latham, D.G. Dunlop, R.O. Oreffo, Bone and metal: an orthopaedic perspective on osseointegration of metals, Acta Biomater. 10 (2014) 4043–4057, https://doi.org/10.1016/j.actbio.2014.06.004

[122] A. Al-Mayouf, A. Al-Swayih, N. Al-Mobarak, A. Al-Jabab, Corrosion behavior of a new titanium alloy for dental implant applications in fluoride media, Mater. Chem. Phys. 86 (2004) 320–329, https://doi.org/10.1016/j.matchemphys.2004.03.019

[123] D. Cadosch, E. Chan, O.P. Gautschi, L. Filgueira, Metal is not inert: Role of metal ions released by biocorrosion in aseptic loosening: current concepts, J. Biomed. Mater. Res. A 91 (2009) 1252–1262, https://doi.org/10.1002/jbm.a.32625

[124] V.C. Mendes, R. Moineddin, J.E. Davies, Discrete calcium phosphate nanocrystalline deposition enhances osteoconduction on titanium-based implant surfaces, J. Biomed. Mater. Res. A 90 (2009) 577–585, https://doi.org/10.1002/jbm.a.32126

[125] H. Kajiwara, T. Yamaza, M. Yoshinari, T. Goto, S. Iyama, I. Atsuta, M.A. Kido, T. Tanaka, The bisphosphonate pamidronate on the surface of titanium

stimulates bone formation around tibial implants in rats, Biomaterials 26 (2005) 581–587, https://doi.org/10.1016/j.biomaterials.2004.02.072
[126] E.P. Chan, A. Mhawi, P. Clode, M. Saunders, L. Filgueira, Effects of titanium (IV) ions on human monocyte-derived dendritic cells, Metallomics 1 (2009) 166–174, https://doi.org/10.1039/b820871a
[127] M.F. López, J.A. Jiménez, A. Gutierrez, Corrosion study of surface-modified vanadium-free titanium alloys, Electrochim. Acta 48 (2003) 1395–1401, https://doi.org/10.1016/S0013-4686(03)00006-9
[128] M.A. McGee, D.W. Howie, K. Costi, D.R. Haynes, C.I. Wildenauer, M.J. Pearcy, J.D. McLean, Implant retrieval studies of the wear and loosening of prosthetic joints: a review, Wear 241 (2000) 158–165, https://doi.org/10.1016/S0043-1648(00)00370-7
[129] Q. Jia, Y. Cui, R. Yang, A study of two refractories as mould materials for investment casting TiAl based alloys, J. Mater. Sci. 41 (2006) 3045–3049, https://doi.org/10.1007/s10853-006-6785-3
[130] U. Kattner, J.-C. Lin, Y. Chang, Thermodynamic assessment and calculation of the Ti-Al system, Metall. Trans. A 23 (1992) 2081–2090, https://doi.org/10.1007/BF02646001
[131] B. Choi, S. Lee, Y. Kim, Influence of TiO_2 on alpha case reaction of Al_2O_3 mould in Ti investment casting, Mater. Sci. Technol. 29 (2013) 1453–1462, https://doi.org/10.1179/1743284713Y.0000000296
[132] E. Zhou, C. Suryanarayana, F.H. s. Froes, Effect of premilling elemental powders on solid solubility extension of magnesium in titanium by mechanical alloying, Mater. Lett. 23 (1995) 27–31, https://doi.org/10.1016/0167-577X(95)00009-7
[133] P. Chartrand, A.D. Pelton, Critical evaluation and optimization of the thermodynamic properties and phase diagrams of the Al-Mg, Al-Sr, Mg-Sr, and Al-Mg-Sr systems, J. Phase Equilib. Diffus. 15 (1994) 591–605, https://doi.org/10.1007/BF02647620
[134] Y.-W. Chang, C.-C. Lin, Compositional dependence of phase formation mechanisms at the interface between titanium and calcia-stabilized zirconia at 1550 °C, J. Am. Ceram. Soc. 93 (2010) 3893–3901.
[135] R. Domagala, S. Lyon, R. Ruh, The pseudobinary Ti-ZrO2, J. Am. Ceram. Soc. 56 (1973) 584–587, https://doi.org/10.1111/j.1151-2916.1973.tb12421.x
[136] J. Murray, The Ti-Zr (titanium-zirconium) system, Bull. Alloy Phase Diagr. 2 (1981) 197–201, https://doi.org/10.1007/BF02881478
[137] W. Kroll, Einige Eigenschaften des reinen Titans, Metallwirtschaft 18 (1939) 77–80.
[138] M. Hillert, X. Wang, Thermodynamic calculation of the CaO - MgO system, Calphad 13 (1989) 267–271, https://doi.org/10.1016/0364-5916(89)90006-0
[139] T. Degawa, G. Okuyama, A. Hashimoto, S. Uchida, K. Fujiwara, M. Ebata, T. Satou, T. Ototani, Method for melting Ti or a high Ti alloy in CaO refractories, 1987. USA Patent 4,710,481.
[140] B. Friedrich, J. Morscheiser, C. Lochbichler, Potential of ceramic crucibles for melting of titanium-alloys and gamma-titaniumaluminide, in: 51st International Colloqium on Refractories, 2008, pp. 229–232.
[141] Z. Li, S. Zhang, W. Lee, Improving the hydration resistance of lime-based refractory materials, Int. Mater. Rev. 53 (2008) 1–20, https://doi.org/10.1179/174328007×212508
[142] T. Nielsen, M. Leipold, Thermal expansion in air of ceramic oxides to 2200 °C, J. Am. Ceram. Soc. 46 (1963) 381–387, https://doi.org/10.1111/j.1151-2916.1963.tb11756.x
[143] Y. Xia, Z.Z. Fang, P. Sun, Y. Zhang, T. Zhang, M. Free, The effect of molten salt on oxygen removal from titanium and its alloys using calcium, J. Mater. Sci. 52 (2017) 4120–4128, https://doi.org/10.1007/s10853-016-0674-1
[144] G.Z. Chen, D.J. Fray, T.W. Farthing, Direct electrochemical reduction of titanium dioxide to titanium in molten calcium chloride, Nature 407 (2000) 361–364, https://doi.org/10.1038/35030069
[145] M. Ma, D. Wang, W. Wang, X. Hu, X. Jin, G.Z. Chen, Extraction of titanium from different titania precursors by the FFC cambridge process, J. Alloy. Compd. 420 (2006) 37–45, https://doi.org/10.1016/j.jallcom.2005.10.048
[146] C. Schwandt, D. Fray, Determination of the kinetic pathway in the electrochemical reduction of titanium dioxide in molten calcium chloride, Electrochim. Acta 51 (2005) 66–76, https://doi.org/10.1016/j.electacta.2005.03.048
[147] D. Alexander, C. Schwandt, D. Fray, The electro-deoxidation of dense titanium dioxide precursors in molten calcium chloride giving a new reaction pathway, Electrochim. Acta 56 (2011) 3286–3295, https://doi.org/10.1016/j.electacta.2011.01.027
[148] X. Yan, D. Fray, Production of niobium powder by direct electrochemical reduction of solid Nb_2O_5 in a eutectic $CaCl_2$-NaCl melt, Met. Mater. Trans. B 33 (2002) 685–693, https://doi.org/10.1007/s11663-002-0021-6
[149] E. Gordo, G.Z. Chen, D.J. Fray, Toward optimisation of electrolytic reduction of solid chromium oxide to chromium powder in molten chloride salts, Electrochim. Acta 49 (2004) 2195–2208, https://doi.org/10.1016/j.electacta.2003.12.045
[150] S. Schafföner, Calcium Zirconate as a Refractory Material for Titanium and Titanium Alloy Melts (Ph.D. thesis), Technische Universität Bergakademie Freiberg, 2015.
[151] C.-H. Li, J. He, Z. Zhang, B. Yang, H.-Y. Leng, X.-G. Lu, Z.-L. Li, Z. Wu, H.-B. Wang, Preparation of TiFe based alloys melted by CaO crucible and its hydrogen storage properties, J. Alloy. Compd. 618 (2015) 679–684, https://doi.org/10.1016/j.jallcom.2014.08.154
[152] Q. Jia, Y. Cui, R. Yang, Intensified interfacial reactions between gamma titanium aluminide and CaO stabilised ZrO_2, Int. J. Cast Met. Res. 17 (2004) 23–28, https://doi.org/10.1179/136404604225014800
[153] J. Barbosa, H. Puga, C.S. Ribeiro, O. Teodoro, A.C. Monteiro, Characterisation of metal/mould interface on investment casting of γ-TiAl, Int. J. Cast Met. Res. 19 (2006) 331–338, https://doi.org/10.1179/136404606×163497
[154] J. Barbosa, C.S. Ribeiro, A.C. Monteiro, Influence of superheating on casting of γ-TiAl, Intermetallics 15 (2007) 945–955.
[155] R. Cui, M. Gao, H. Zhang, S. Gong, Interactions between TiAl alloys and yttria refractory material in casting process, J. Mater. Process. Technol. 210 (2010) 1190–1196, https://doi.org/10.1016/j.jmatprotec.2010.03.003
[156] C.-C. Lin, Y.-W. Chang, K.-L. Lin, K.-F. Lin, Effect of yttria on interfacial reactions between titanium melt and hot-pressed yttria/zirconia composites at 1700 °C, J. Am. Ceram. Soc. 91 (2008) 2321–2327, https://doi.org/10.1111/j.1551-2916.2008.02428.x
[157] R. Cui, H. Zhang, X. Tang, L. Ma, H. Zhang, S. Gong, Interactions between γ -TiAl melt and Y_2O_3 ceramic material during directional solidification process, Trans. Nonferr. Met. Soc. China 21 (2011) 2415–2420.
[158] X. Cheng, C. Yuan, S. Blackburn, P. Withey, The study of the influence of binder systems in an Y_2O_3-ZrO_2 facecoat material on the investment casting slurries and shells properties, J. Eur. Ceram. Soc. 34 (2014) 3061–3068, https://doi.org/10.1016/j.jeurceramsoc.2014.03.005
[159] Y.-S. Cui, D.-B. Liu, L.-H. Chai, Z.-Y. Chen, Interface reactions between TiAl alloys and diacetatozirconic acid-yttria molds differentiated by ammonium metatungstate addition, Rare Met. (2017) 1–6, https://doi.org/10.1007/s12598-016-0875-4
[160] Y. Cui, X. Tang, M. Gao, L. Ma, Z. Hu, Interactions between TiAl alloy and different oxide moulds under high-temperature and long-time condition, High Temp. Mater. Process. 32 (2013) 295–302, https://doi.org/10.1515/htmp-2012-0120
[161] M. Gao, R.-J. Cui, L. Ma, H. Zhang, X. Tang, H. Zhang, Physical erosion of yttria crucibles in Ti-54Al alloy casting process, J. Mater. Process. Technol. 211 (2011) 2004–2011, https://doi.org/10.1016/j.jmatprotec.2011.06.021
[162] T. Tetsui, T. Kobayashi, T. Mori, T. Kishimoto, H. Harada, Evaluation of yttria applicability as a crucible for induction melting of TiAl alloy, Mater. Trans. 51 (2010) 1656–1662, https://doi.org/10.2320/matertrans.MAW201002
[163] R. Saha, T. Nandy, R. Misra, K. Jacob, On the evaluation of stability of rare earth oxides as face coats for investment casting of titanium, Metall. Trans. B 21 (1990) 559–566, https://doi.org/10.1007/BF02667869
[164] R. Helferich, C. Zanis, An Investigation of Yttrium Oxide as a Crucible Material for Melting Titanium, Technical Report, David W. Taylor Naval Ship Research and Development Center, Annapolis, MD, 1973.
[165] A. Szkliniarz, W. Szkliniarz, Assessment of quality of Ti alloys melted in induction furnace with ceramic crucible, Solid State Phenomena 176 Trans Tech Publications, 2011, pp. 139–148, https://doi.org/10.4028/www.scientific.net/ssp.176.139
[166] Y. Du, Z. Jin, P. Huang, Thermodynamic calculation of the zirconia-calcia system, J. Am. Ceram. Soc. 75 (1992) 3040–3048.
[167] S. Schafföner, C.G. Aneziris, H. Berek, J. Hubálková, A. Priese, Fused calcium zirconate for refractory applications, J. Eur. Ceram. Soc. 33 (2013) 3411–3418, https://doi.org/10.1016/j.jeurceramsoc.2013.07.008
[168] G. Chen, J. Kang, P. Gao, Z. Qin, X. Lu, C. Li, Dissolution of $BaZrO_3$ refractory in titanium melt, Int. J. Appl. Ceram. Technol. 15 (2018) 1459–1466, https://doi.org/10.1111/ijac.13009
[169] G. Chen, B. Lan, F. Xiong, P. Gao, H. Zhang, X. Lu, C. Li, Pilot-scale experimental evaluation of induction melting of Ti-46Al-8Nb alloy in the fused $BaZrO_3$ crucible, Vacuum 159 (2019) 293–298, https://doi.org/10.1016/j.vacuum.2018.10.050
[170] S. Stølen, T. Grande, Chemical Thermodynamics of Materials: Macroscopic and Microscopic Aspects, John Wiley & Sons, 2004, p. 285 327-8, 347.
[171] M. De Graef, M.E. McHenry, Structure of Materials: An Introduction to Crystallography, Diffraction and Symmetry, Cambridge University Press, 2012, pp. 561–596.
[172] C.B. Carter, M.G. Norton, Ceramic Materials: Science and Engineering 716 Springer, 2007, pp. 87–117.
[173] D. Poirier, G. Geiger, Transport Phenomena in Materials Processing, Springer, 2016, pp. 419–461.
[174] S. Schafföner, C.G. Aneziris, H. Berek, J. Hubálková, B. Rotmann, B. Friedrich, Corrosion behavior of calcium zirconate refractories in contact with titanium aluminide melts, J. Eur. Ceram. Soc. 35 (2015) 1097–1106, https://doi.org/10.1016/j.jeurceramsoc.2014.09.032
[175] R. Gaddam, B. Sefer, R. Pederson, M.-L. Antti, Study of alpha-case depth in Ti-6Al-2Sn-4Zr-2Mo and Ti-6Al-4V, IOP Conf. Ser. Mater. Sci. Eng. 48 (2013) 012002, https://doi.org/10.1088/1757-899x/48/1/012002
[176] B. Sefer, R. Gaddam, J.J. Roa, A. Mateo, M.-L. Antti, R. Pederson, Chemical milling effect on the low cycle fatigue properties of cast Ti-6Al-2Sn-4Zr-2Mo alloy, Int. J. Fatigue 92 (2016) 193–202, https://doi.org/10.1016/j.ijfatigue.2016.07.003